

# Charmless $B \rightarrow PV, VV$ decays and new physics effects in the mSUGRA model

Wenjuan Zou\*

*Department of Physics and Institute of Theoretical Physics,  
Nanjing Normal University, Nanjing, Jiangsu 210097, P.R.China*

Zhenjun Xiao†

*Department of Physics and Institute of Theoretical Physics,  
Nanjing Normal University, Nanjing, Jiangsu 210097, P.R.China and*

*CCAST(World Laboratory), P.O.Box 8730, Beijing 100080, China*

(Dated: June 21, 2021)

## Abstract

By employing the QCD factorization approach, we calculate the new physics contributions to the branching ratios of the two-body charmless  $B \rightarrow PV$  and  $B \rightarrow VV$  decays in the framework of the minimal supergravity (mSUGRA) model. we choose three typical sets of the mSUGRA input parameters in which the Wilson coefficient  $C_{7\gamma}(m_b)$  can be either SM-like ( the case A and C) or has a flipped-sign (the case B). We found numerically that (a) the SUSY contributions are always very small for both case A and C; (b) for those tree-dominated decays, the SUSY contributions in case B are also very small; (c) for those QCD penguin-dominated decay modes, the SUSY contributions in case B can be significant, and can provide an enhancement about 30%  $\sim$  260% to the branching ratios of  $B \rightarrow K^*(\pi, \phi, \rho)$  and  $K\phi$  decays, but a reduction about 30%  $\sim$  80% to  $B \rightarrow K(\rho, \omega)$  decays; and (d) the large SUSY contributions in the case B may be masked by the large theoretical errors dominated by the uncertainty from our ignorance of calculating the annihilation contributions in the QCD factorization approach.

PACS numbers: 13.25.Hw, 12.15.Ji, 12.60.Jv, 14.40.Nd

---

\*Electronic address: zouwenjuan@email.njnu.edu.cn

†Electronic address: xiaozhenjun@njnu.edu.cn

## I. INTRODUCTION

Along with the excellent performance of the B factory experiments [1, 2] and the forthcoming LHCb and other B meson related experiments[3], huge amount of B data with great precision are expected in the following five to ten years. The precision measurements of the B meson system can provide an insight into very high energy scales via the indirect loop effects of the new physics beyond the standard model (SM) [4, 5]. Although currently available data agree well with the SM predictions when considering the still large uncertainties both in theory and experiments, we generally believe that the B-factories can at least detect the first signals of new physics if it is there.

As for the charmless hadronic two-body B decays considered here, people indeed have found some deviations from the SM expectations, such as the unexpected large branching ratios of  $B \rightarrow K\eta'$  and  $B \rightarrow \pi^0\pi^0$  decay modes, the " $K\pi$ " puzzle [5, 6] and the so-called  $\phi K_s$  anomaly at  $3.8\sigma$  level [7]. Although not convincing, these potential deviations may be considered as the first hints of new physics beyond the SM in B meson experiments.

On the theory side, by employing the low energy effective Hamiltonian and various factorization hypothesis the charmless B meson decays have been widely studied in the framework of the SM [8, 9, 10, 11, 12, 13, 14]. The possible new physics contributions to B meson decays induced by loop diagrams involving various new particles have been studied extensively, for example, in the Technicolor models[15], the two-Higgs-doublet models[16, 17] and the supersymmetric models [18, 19, 20, 21, 22].

Among the various new physics models, the minimal supergravity (mSUGRA) model [23] is a constrained minimal supersymmetric standard model [24] which has only five free parameters (  $\tan\beta, m_{\frac{1}{2}}, m_0, A_0$ , and  $sign(\mu)$  ) at the high energy scale. In Refs. [18, 19, 20, 25], for example, the authors studied the rare decays  $B \rightarrow X_s\gamma$ ,  $B \rightarrow X_s l\bar{l}$ ,  $B \rightarrow l^+l^-$  and the  $B^0 - \bar{B}^0$  mixing in the mSUGRA model, and found some constraints on the parameter space of this model.

In a recent paper[26], we calculated the SUSY contributions to the branching ratios of the twenty one  $B \rightarrow PP$  (P stands for pseudo-scalar light meson) decay modes in the mSUGRA model by employing the QCD factorization approach. We deduced analytically the contributions given by the new penguin diagrams induced by gluinos, charged-Higgs bosons, charginos and neutralinos, and obtained the analytical expressions of the SUSY corrections to the Wilson coefficients. By considering the current constraints, such as the branching ratio of the inclusive radiative B-decay,  $C_{7\gamma}(m_b)$  can be either SM-like or sign-flipped comparing with that in the SM. At the considered parameter point where the SUSY contributions can make the sign of  $C_{7\gamma}(m_b)$  reversed with respect to the SM one, we found that (a) the SUSY corrections to the Wilson coefficients  $C_{7\gamma}(M_W)$  and  $C_{8g}(M_W)$  can be rather large; (b) the SUSY enhancements to those penguin-dominated decays can be as large as 30%-50%; (c)for  $B \rightarrow K\pi$  decays, the inclusion of the SUSY enhancements can improve the consistency of the theoretical prediction with the data; and (d) the large SUSY contributions to  $B \rightarrow K\eta'$  decays will help us to give a new physics interpretation for the so-called " $K\eta'$ " puzzle.

In this paper, we will extend the previous work [26] to the cases for thirty nine  $B \rightarrow PV$  decays and nineteen  $B \rightarrow VV$  decay modes (here V stands for the light vector meson). This paper is organized as follows. In Sec. II and Sec. III, we give a brief review for the mSUGRA model and the QCD factorization approach for two-body B meson decays.

In Sec. IV and Sec. V, we present the related formulae and calculate the CP-averaged branching ratios for  $B \rightarrow PV$  and  $B \rightarrow VV$  decays, respectively. The summary and some discussions are included in the final section.

## II. THE MSUGRA MODEL AND THE NEW PHYSICS CONTRIBUTIONS

In this section, we first recapitulate the basic theoretical framework of the mSUGRA model to set up the notation and then calculate the SUSY corrections to the Wilson coefficients in the mSUGRA model.

### A. Outline of the mSUGRA model

The most general superpotential compatible with gauge invariance, renormalizability and R-parity conserving in MSSM can be written as [24]:

$$\mathcal{W} = \varepsilon_{\alpha\beta} \left[ f_{Uij} Q_i^\alpha H_2^\beta U_j + f_{Dij} H_1^\alpha Q_i^\beta D_j + f_{Eij} H_1^\alpha L_i^\beta E_j - \mu H_1^\alpha H_2^\beta \right] \quad (1)$$

Where  $Q, U, D, L, E, H_1$  and  $H_2$  are chiral superfields.  $f_D, f_U$  and  $f_E$  are Yukawa coupling constants for down-type, up-type quarks, and leptons, respectively. The suffixes  $\alpha, \beta = 1, 2$  are SU(2) indices and  $i, j = 1, 2, 3$  are generation indices.  $\varepsilon_{\alpha\beta}$  is the antisymmetric tensor with  $\varepsilon_{12} = 1$ .

In addition to the SUSY invariant terms, a set of terms which explicitly but softly break SUSY should be added to the supersymmetric Lagrangian. A general form of the soft SUSY-breaking terms is given as:

$$\begin{aligned} -\mathcal{L}_{soft} = & (m_Q^2)_{ij} \tilde{q}_{Li}^+ \tilde{q}_{Lj} + (m_U^2)_{ij} \tilde{u}_{Ri}^* \tilde{u}_{Rj} + (m_D^2)_{ij} \tilde{d}_{Ri}^* \tilde{d}_{Rj} + (m_L^2)_{ij} \tilde{l}_{Li}^+ \tilde{l}_{Lj} \\ & + (m_E^2)_{ij} \tilde{e}_{Ri}^* \tilde{e}_{Rj} + \Delta_1^2 h_1^+ h_1 + \Delta_2^2 h_2^+ h_2 \\ & + \varepsilon_{\alpha\beta} \left[ A_{Uij} \tilde{q}_{Li}^\alpha h_2^\beta \tilde{u}_{Rj}^* + A_{Dij} h_1^\alpha \tilde{q}_{Li}^\beta \tilde{d}_{Rj}^* + A_{Eij} h_1^\alpha \tilde{l}_{Li}^\beta \tilde{e}_{Rj}^* + B \mu h_1^\alpha h_2^\beta \right] \\ & + \frac{1}{2} m_{\tilde{B}} \tilde{B} \tilde{B} + \frac{1}{2} m_{\tilde{W}} \tilde{W} \tilde{W} + \frac{1}{2} m_{\tilde{G}} \tilde{G} \tilde{G} + H.C. \end{aligned} \quad (2)$$

where  $\tilde{q}_{Li}, \tilde{u}_{Ri}^*, \tilde{d}_{Ri}^*, \tilde{l}_{Li}, \tilde{e}_{Ri}^*$ , and  $h_1$  and  $h_2$  are scalar components of chiral superfields  $Q_i, U_i, D_i, L_i, E_i, H_1$ , and  $H_2$  respectively, and  $\tilde{B}, \tilde{W}$ , and  $\tilde{G}$  are  $U(1)_Y, SU(2)_L$ , and  $SU(3)_C$  gauge fermions. And the terms appeared in Eq.(2) are the mass terms for the scalar fermions, mass and bilinear terms for the Higgs bosons, trilinear coupling terms between sfermions and Higgs bosons, and mass terms for the gluinos, Winos and binos, respectively.

In the mSUGRA model, a set of assumptions are added to the MSSM. One underlying assumption is that SUSY-breaking occurs in a hidden sector which communicates with the visible sector only through gravitational interactions. The free parameters in the MSSM

are assumed to obey a set of boundary conditions at the Plank or GUT scale:

$$\begin{aligned}
\alpha_1 &= \alpha_2 = \alpha_3 = \alpha_X, \\
(m_Q^2)_{ij} &= (m_U^2)_{ij} = (m_D^2)_{ij} = (m_L^2)_{ij} = (m_E^2)_{ij} = (m_0^2)\delta_{ij}, \\
\Delta_1^2 &= \Delta_2^2 = m_0^2, \\
A_{Uij} &= f_{Uij}A_0, \quad A_{Dij} = f_{Dij}A_0, \quad A_{Eij} = f_{Eij}A_0, \\
m_{\tilde{B}} &= m_{\tilde{W}} = m_{\tilde{G}} = m_{\frac{1}{2}}
\end{aligned} \tag{3}$$

where  $\alpha_i = g_i^2/(4\pi)$ , while  $g_i$  ( $i=1,2,3$ ) denotes the coupling constant of the  $U(1)_Y$ ,  $SU(2)_L$ ,  $SU(3)_C$  gauge group, respectively. The unification of them is verified according to the experimental results from LEP1[27] and can be fixed at the Grand Unification Scale  $M_{GUT} \sim 2 \times 10^{16} \text{ GeV}$ .

Besides the three parameters  $m_{\frac{1}{2}}$ ,  $m_0$  and  $A_0$ , the bilinear coupling  $B$  and the supersymmetric Higgs(ino) mass parameter  $\mu$  in the supersymmetric sector should be determined. By requiring the radiative electroweak symmetry-breaking (EWSB) takes place at the low energy scale, both of them are obtained except for the sign of  $\mu$ . At this stage, only four continuous free parameters and an unknown sign are left in the mSUGRA model [28]:

$$\tan \beta, m_{\frac{1}{2}}, m_0, A_0, \text{sign}(\mu) \tag{4}$$

In present analysis, we assume that they are all real parameters. Therefore there are no new CP-violating complex phase introduced other than that in the Cabbibo-Kabayashi-Maskawa(CKM) quark mixing matrix [29]. Once the five free parameters of the mSUGRA model are determined, all other parameters at the electroweak scale are then obtained through the GUT universality condition and the renormalization group equation (RGE) evolution. Like in Ref. [26], we here also use the Fortran code - Suspect version 2.1 [30]- to calculate the SUSY and Higgs particle spectrum <sup>1</sup>.

## B. New physics effects in the mSUGRA model

As is well-known, the low energy effective Hamiltonian for the quark level three-body decay  $b \rightarrow qq'q'$  ( $q \in \{d, s\}, q' \in \{u, c, d, s, b\}$ ) at the scale  $\mu \sim m_b$  reads

$$\begin{aligned}
\mathcal{H}_{eff} &= \frac{G_F}{\sqrt{2}} \left\{ \sum_{i=1}^2 C_i(\mu) [V_{ub}V_{uq}^* O_i^u(\mu) + V_{cb}V_{cq}^* O_i^c(\mu)] \right. \\
&\quad \left. - V_{tb}V_{tq}^* \sum_{j=3}^{10} C_j(\mu) O_j(\mu) - V_{tb}V_{tq}^* [C_{7\gamma}(\mu) O_{7\gamma}(\mu) + C_{8g}(\mu) O_{8g}(\mu)] \right\} \tag{5}
\end{aligned}$$

where  $V_{pb}V_{pq}^*$  with  $q = d, s$  is the products of elements of the CKM matrix [29]. The definitions and the explicit expressions of the operators  $O_i$  ( $i = 1 \sim 10, 7\gamma, 8g$ ) and the corresponding Wilson coefficients  $C_i$  can be found in Ref. [31]. In the SM, the Wilson

---

<sup>1</sup> For more details, one can see discussions in Ref. [26] and references therein.

coefficients appeared in eq.(5) are currently known at next-to-leading order (NLO) and can be found easily in Ref. [31].

In the mSUGRA model, the new physics effects on the rare B meson decays will manifest themselves through two channels.

- The new physics contributions to the Wilson coefficients of the same operators involved in the SM calculation;
- The other is the new physics contributions to the Wilson coefficients of the new operators such as the operators with opposite chiralities with  $O_i$  appeared in eq.(5).

In the SM, the latter is absent because they are suppressed by the ratio  $m_s/m_b$ . In the mSUGRA model, they can also be negligible, as shown in Ref. [32]. Therefore we here use the same operator base as in the SM.

It is well known that there is no SUSY contributions to the Wilson coefficients at the tree level. At the one-loop level, there are four kinds of SUSY contributions to the quark level decay process  $b \rightarrow qq' \bar{q}'$ , depending on specific particles propagated in the loops:

- (i) the charged Higgs boson  $H^\pm$  and up-type quarks  $u, c, t$ ;
- (ii) the charginos  $\tilde{\chi}_{1,2}^\pm$  and the scalar up-type quarks  $\tilde{u}, \tilde{c}, \tilde{t}$ ;
- (iii) the neutralinos  $\tilde{\chi}_{1,2,3,4}^0$  and the scalar down-type quarks  $\tilde{d}, \tilde{s}, \tilde{b}$ ;
- (iv) the gluinos  $\tilde{g}$  and the scalar down-type quarks  $\tilde{d}, \tilde{s}, \tilde{b}$ .

In Ref. [26], we have given a detailed derivation of the lengthy expressions of SUSY corrections induced by those penguin diagrams involving SUSY particles to the Wilson coefficients.

In the mSUGRA model, there are five free parameters:  $\tan\beta, m_{\frac{1}{2}}, m_0, A_0$  and  $sign(\mu)$ . Before we calculate the new physics contributions to the considered  $B \rightarrow PV, VV$  decays, we have to check the experimental bounds on these parameters, which have been studied extensively by many authors [33, 34, 35, 36]. The supersymmetry parameter analysis(SPA) project with the main target of high-precision determination of the supersymmetry Lagrangian parameters at the electroweak scale, for example, is under way now [35]. By confronting the precision electroweak data provided by the LEP experiments with the theoretical predictions within the mSUGRA model, the strong constraints on the parameter space have been obtained [33, 34, 35, 36].

From the well measured  $B \rightarrow X_s \gamma$  decays, the magnitude-but not the sign- of the Wilson coefficient  $C_{7\gamma}(m_b)$  is strongly constrained. This is an important constraint. However, various new physics can change the sign of  $C_{7\gamma}(m_b)$  without changing the branching ratio of  $B \rightarrow X_s \gamma$  decay obviously.

From the measurements of the  $b \rightarrow sl^+l^-$  decays, one can determine the relative sign of the Wilson coefficients as well as their absolute values. The latest Belle and BaBar measurements of the inclusive  $B \rightarrow X_s l^+l^-$  branching ratios indicated that the sign of  $C_{7\gamma}(m_b)$  is unlikely to be different from that in the SM [37]. On the other hand, the studies [37, 38] also show that a positive  $C_{7\gamma}^{eff}$  could be made compatible with experiments only by large  $\mathcal{O}(1)$  new physics corrections to  $C_{9,10}^{eff}$ , while the SM values of  $C_{9,10}^{eff}$  are around +4.2 and -4.4 respectively.

TABLE I: Three typical sets of SUSY parameters to be used in numerical calculation. The third case is the “typical” mSUGRA point “SPS 1b” as defined in Ref.[36]. The last column show the values of the ratio  $R_7 = C_{7\gamma}(m_b)/C_{7\gamma}^{SM}(m_b)$ . All masses are in units of  $GeV$ .

| CASE | $m_0$ | $m_{\frac{1}{2}}$ | $A_0$ | $\tan\beta$ | $Sign[\mu]$ | $R_7$ |
|------|-------|-------------------|-------|-------------|-------------|-------|
| A    | 300   | 300               | 0     | 2           | −           | 1.10  |
| B    | 369   | 150               | −400  | 40          | +           | −0.93 |
| C    | 200   | 400               | 0     | 30          | +           | 0.82  |

For the semi-leptonic Wilson coefficients  $C_9$  and  $C_{10}$  in the minimal supergravity model, the authors of Ref. [20] have made a detailed analysis and found that  $C_9(m_b)$  and  $C_{10}(m_b)$  differ from their SM values by at most 5% in the parameter space for  $-2 \leq C_{7\gamma}(m_b)/C_{7\gamma}^{SM}(m_b) \leq 2$  and for  $\tan\beta = 3, 30$ . This result supports a SM-like  $C_{7\gamma}(m_b)$  in the mSUGRA model.

This August, Belle Collaboration reported their measurement of the ratios of Wilson coefficients  $A_9/A_7$  and  $A_{10}/A_7$ <sup>2</sup> in  $B \rightarrow K^* l^+ l^-$  decay [40]. They exclude a positive  $A_9 A_{10}$  at more than 95% CL., but can not determine the sign of  $A_7$  (i.e.  $C_{7\gamma}(m_b)$ ).

Based on a lot of previous studies about the constraints on the parameter space of the mSUGRA model [26, 33, 34, 35, 36, 38], we can choose several typical sets of input parameters to show the pattern of the new physics corrections to the branching ratios of the studied decays in the mSUGRA model. In Ref. [26] we selected two sets of input parameters (case-A and case-B) and found that (a) the SUSY corrections to the Wilson coefficients  $C_k (k = 3 \sim 6)$  are always very small and can be neglected safely; (b) with the inclusion of SUSY corrections, the Wilson coefficient  $C_{7\gamma}(m_b)$  remained SM-like for case-A, but changed its sign for the case-B. Numerical results for the branching ratios of  $B \rightarrow PP$  decays also show that the new physics corrections are very small for the case-A, but can be significant for the case-B.

In this paper, besides the choice of case-A and B as defined in Ref.[26], we also consider the third case, the case-C, which is the “typical” mSUGRA point “SPS 1b” as defined in Ref.[36]. In the case-C, the SUSY corrections to  $C_k (k = 3 \sim 6)$  are also negligibly small, while  $C_{7\gamma}(m_b)$  is SM-like after the inclusion of SUSY contributions. The three sets of mSUGRA input parameters to be used in numerical calculations here are listed in Table I, the numerical values of the ratio  $R_7 = C_{7\gamma}(m_b)/C_{7\gamma}^{SM}(m_b)$  for each cases are also given in the table. It is easy to see that the Wilson coefficient  $C_{7\gamma}$  in the mSUGRA model is SM-like (negative) for both case-A and C, but nonstandard (positive) for case-B. The

<sup>2</sup> At next-next-to-leading order (NNLO), the effective Wilson coefficients  $C_{7\gamma}^{eff}$ ,  $C_9^{eff}$  and  $C_{10}^{eff}$  have many small high order correction terms [39], one usually use the leading coefficients  $A_7$ ,  $A_9$  and  $A_{10}$  in the evaluations [40]. The numerical differences between  $C_{7\gamma,9,10}^{eff}$  and  $A_{7,9,10}$  are indeed very small. It is worth noting that, instead of the (electroweak penguin) coefficients  $C_9$  and  $C_{10}$  as defined in Eq.(5), the coefficients  $C_9^{eff}$  and  $C_{10}^{eff}$  here correspond to the low-energy interaction terms  $(\bar{s}_L \gamma_\mu b_L)(\bar{l} \gamma^\mu l)$  and  $(\bar{s}_L \gamma_\mu b_L)(\bar{l} \gamma^\mu \gamma_5 l)$ , respectively.

ratio  $R_7 \gtrsim 1$  for case-A, but  $\lesssim 1$  for the case-C, due to the strong bound imposed by the precision data of  $B \rightarrow X_s \gamma$ .

From above discussions, one expects that the case-A and C will be very similar phenomenologically. The numerical calculations to be given in the following sections indeed show that the theoretical predictions for the branching ratios in case-A and C are almost identical with each other: the difference is less than 2%. We therefore will present the numerical results of the branching ratios explicitly for case-B and case-C only, and compare them with the corresponding SM predictions.

### III. $B \rightarrow M_1 M_2$ DECAYS IN THE QCD FACTORIZATION APPROACH

In QCD factorization approach, when the final state hadrons of B meson two-body decays are all light mesons (mesons composed of light  $u, d$ , or  $s$  quarks, and with a mass of order  $\Lambda_{QCD}$ ), the matrix element of each operator in the effective Hamiltonian  $\mathcal{H}_{eff}$  can be written as [13]

$$\begin{aligned} \langle M_1 M_2 | O_i | B \rangle = & \sum_j F_j^{B \rightarrow M_1} \int_0^1 dx T_{ij}^I(x) \Phi_{M_2}(x) + (M_1 \leftrightarrow M_2) \\ & + \int_0^1 d\xi \int_0^1 dx \int_0^1 dy T_i^{II}(\xi, x, y) \Phi_B(\xi) \Phi_{M_1}(x) \Phi_{M_2}(y) \end{aligned} \quad (6)$$

where  $F_j^{B \rightarrow M_1}$  is the form factor describing  $B \rightarrow M_1$  decays,  $T_{ij}^I$  and  $T_i^{II}$  denote the perturbative short-distance interactions and can be calculated by the perturbation approach, and  $\Phi_X(x)$  ( $X = B, M_{1,2}$ ) are the universal and nonperturbative light-cone distribution amplitudes (LCDA) for the heavy B meson and the light  $M_{1,2}$  meson respectively. Weak annihilation effects which are suppressed by  $\Lambda_{QCD}/m_b$  are not included in Eq.(6).

Considering the low energy effective Hamiltonian Eq.(5) and the QCDF formula Eq.(6), the decay amplitude can be written as

$$\mathcal{A}^f(B \rightarrow M_1 M_2) = \frac{G_F}{\sqrt{2}} \sum_{p=u,c} \sum_i V_{pb} V_{pq}^* a_i^p(\mu) \langle M_1 M_2 | O_i | B \rangle_F. \quad (7)$$

Here  $\langle M_1 M_2 | O_i | B \rangle_F$  is the factorized matrix element. The explicit expressions for the decay amplitudes of  $B \rightarrow M_1 M_2$  decays can be found for example in the Appendixes of Refs. [8, 9]. Following Beneke *et al.* [13], the coefficients  $a_i(M_1 M_2)$  ( $i = 1$  to 10) in Eq.(7) with  $M_1$  absorbing the spectator quark is

$$\begin{aligned} a_i^p(M_1 M_2) = & (C_i + \frac{C_{i\pm 1}}{N_c}) N_i(M_2) \\ & + \frac{C_{i\pm 1}}{N_c} \frac{C_F \alpha_s}{4\pi} \left[ V_i(M_2) + \frac{4\pi^2}{N_c} H_i(M_1 M_2) \right] + P_i^p(M_2), \end{aligned} \quad (8)$$

where the upper (lower) signs apply when  $i$  is odd (even). The functions  $V_i(M_2)$  account for one loop vertex corrections,  $H_i(M_1 M_2)$  for hard spectator interactions and  $P_i^p(M_2)$  for penguin contributions. The explicit expressions for these functions can be found in Ref. [13].

As mentioned previously, the SUSY contributions to the Wilson coefficients of the four-quark penguin operators are very small and have been neglected. The new magnetic penguin contributions in the mSUGRA model can manifest themselves as radiative corrections to the coefficients  $a_i^p$  and be contained in the functions  $P_i^p(M_2)$ , which is present only for  $i = 4, 6, 8, 10$  [13]. To make this visible, here we just show the functions  $P_4^p(M_2)$  and  $P_{10}^p(M_2)$ . At order  $\alpha_s$ , these two functions are

$$\begin{aligned}
P_4^p(M_2) = & \frac{C_F \alpha_s}{4\pi N_c} \left\{ C_1 \left[ \frac{4}{3} \ln \frac{m_b}{\mu} + \frac{2}{3} - G_{M_2}(s_p) \right] \right. \\
& + C_3 \left[ \frac{8}{3} \ln \frac{m_b}{\mu} + \frac{4}{3} - G_{M_2}(0) - G_{M_2}(1) \right] \\
& + (C_4 + C_6) \left[ \frac{4n_f}{3} \ln \frac{m_b}{\mu} - (n_f - 2)G_{M_2}(0) - G_{M_2}(s_c) - G_{M_2}(1) \right] \\
& \left. - 2C_{8g}^{eff} \int_0^1 \frac{dx}{1-x} \Phi_{M_2}(x) \right\}, \tag{9}
\end{aligned}$$

$$\begin{aligned}
P_{10}^p(M_2) = & \frac{\alpha}{9\pi N_c} \left\{ (C_1 + N_c C_2) \left[ \frac{4}{3} \ln \frac{m_b}{\mu} + \frac{2}{3} - G_{M_2}(s_p) \right] \right. \\
& \left. - 3C_{7\gamma}^{eff} \int_0^1 \frac{dx}{1-x} \Phi_{M_2}(x) \right\}, \tag{10}
\end{aligned}$$

where  $s_u = m_u^2/m_b^2 \approx 0$  and  $s_c = m_c^2/m_b^2$  are mass ratios involved in the evaluation of penguin diagrams.  $\Phi_{M_2}(x)$  is the leading twist LCDA which can be expanded in Gegenbauer polynomials.  $C_{7\gamma}^{eff} = C_{7\gamma} - \frac{1}{3}C_5 - C_6$  and  $C_{8g}^{eff} = C_{8g} + C_5$  are the so-called “effective” Wilson coefficients, where the SUSY contribution is involved. The explicit expressions of the functions  $G_{M_2}(0)$ ,  $G_{M_2}(1)$  and  $G_{M_2}(s_p)$  appeared in Eqs.(9,10) can be found easily in Refs. [11, 13].

When calculating the decay amplitudes, the coefficients  $a_i (i = 3 \sim 10)$  always appear in pairs. So in terms of the coefficients  $a_i^p$ , one can define  $\alpha_i^p$  as follows [13]:

$$\begin{aligned}
\alpha_1(M_1 M_2) &= a_1(M_1 M_2), \\
\alpha_2(M_1 M_2) &= a_2(M_1 M_2), \\
\alpha_3^p(M_1 M_2) &= \begin{cases} a_3^p(M_1 M_2) - a_5^p(M_1 M_2) & \text{if } M_1 M_2 = PP, VP, \\ a_3^p(M_1 M_2) + a_5^p(M_1 M_2) & \text{if } M_1 M_2 = PV, \end{cases} \\
\alpha_4^p(M_1 M_2) &= \begin{cases} a_4^p(M_1 M_2) + r_\chi^{M_2} a_6^p(M_1 M_2) & \text{if } M_1 M_2 = PP, PV, \\ a_4^p(M_1 M_2) - r_\chi^{M_2} a_6^p(M_1 M_2) & \text{if } M_1 M_2 = VP, \end{cases} \tag{11} \\
\alpha_{3,EW}^p(M_1 M_2) &= \begin{cases} a_9^p(M_1 M_2) - a_7^p(M_1 M_2) & \text{if } M_1 M_2 = PP, VP, \\ a_9^p(M_1 M_2) + a_7^p(M_1 M_2) & \text{if } M_1 M_2 = PV, \end{cases} \\
\alpha_{4,EW}^p(M_1 M_2) &= \begin{cases} a_{10}^p(M_1 M_2) + r_\chi^{M_2} a_8^p(M_1 M_2) & \text{if } M_1 M_2 = PP, PV, \\ a_{10}^p(M_1 M_2) - r_\chi^{M_2} a_8^p(M_1 M_2) & \text{if } M_1 M_2 = VP. \end{cases}
\end{aligned}$$



For pseudoscalar meson P and vector meson V, the ratios  $r_\chi^P$  and  $r_\chi^V(\mu)$  are defined as

$$r_\chi^P(\mu) = \frac{2m_P^2}{m_b(\mu)(m_{q_1} + m_{q_2})(\mu)}, \quad (12)$$

$$r_\chi^V(\mu) = \frac{2m_V}{m_b(\mu)} \frac{f_V^\perp(\mu)}{f_V}, \quad (13)$$

where  $m_{q_1}$  and  $m_{q_2}$  are the current masses of the component quarks of P meson, and  $f_V^\perp(\mu)$  is the scale-dependent transverse decay constant of vector meson V. Although all the terms proportional to  $r_\chi^{M_2}$  are formally suppressed by one power of  $\Lambda_{\text{QCD}}/m_b$  in the heavy-quark limit, these terms are chirality enhanced and not always small. They are very important in those penguin-dominant B meson decays, such as the interesting channels  $B \rightarrow K\eta'$ , etc.

In QCD factorization approach, the nonfactorizable power-suppressed contributions are neglected. However, the hard-scattering spectator interactions and annihilation diagrams can not be neglected because of the chiral enhancement. Since they give rise to infrared endpoint singularities when computed perturbatively, they can only be estimated in a model dependent way and with a large uncertainty. In Refs. [11, 13] these contributions are parameterized by two complex quantities,  $\chi_H$  and  $\chi_A$ ,

$$\chi_{H,A} = (1 + \rho_{H,A} e^{i\phi_{H,A}}) \ln \frac{m_B}{\Lambda_h} \quad (14)$$

where  $\Lambda_h = 0.5 \text{ GeV}$ ,  $\phi_{H,A}$  are free phases in the range  $[-180^\circ, 180^\circ]$ , and  $\rho_{H,A}$  are real parameters varying within  $[0, 1]$ . In this paper, we use the same method as in Refs. [11, 13] to estimate these two kinds of contributions.

As given in Ref. [13], the annihilation amplitude can be written as

$$\mathcal{A}^{ann}(B \rightarrow M_1 M_2) \propto \frac{G_F}{\sqrt{2}} \sum_{p=u,c} \sum_i V_{pb} V_{pq}^* f_B f_{M_1} f_{M_2} b_i(M_1 M_2) \quad (15)$$

where  $f_B$  and  $f_M$  are the decay constants of B meson and final-state hadrons respectively. The coefficients  $b_i(M_1 M_2)$  describe the annihilation contributions. For explicit expressions of coefficients  $b_i$ , one can see Refs. [11, 13].

For  $B \rightarrow VV$  decays we have two additional remarks: (a) since  $\langle V|\bar{q}_1 q_2|0 \rangle = 0$ ,  $B \rightarrow VV$  decays do not receive factorizable contribution from  $a_6$  and  $a_8$  penguin terms except for spacelike penguin diagrams; and (b) unlike the PP and PV decay modes, the annihilation amplitude in the VV mode does not have a chiral enhancement of order  $M_B^2/(m_q m_b)$ . Therefore, it is truly power suppressed in heavy quark limit and will be neglected in our calculation. The explicit factorizable coefficients  $a_i$  for  $B \rightarrow VV$  can be found in Ref. [41].

#### IV. BRANCHING RATIOS OF $B \rightarrow PV$ DECAYS

In the following two sections we will calculate the CP-averaged branching ratios for thirty nine  $B \rightarrow PV$  and nineteen  $B \rightarrow VV$  decay modes, respectively. We usually use the central values of the input parameters as collected in Appendix A, and consider the

effects of the uncertainties of these input parameters as specified in the text for individual decay channels.

Theoretically, the branching ratios of charmless decays  $B \rightarrow PV$  in the B meson rest frame can be written as

$$\mathcal{B}r(B \rightarrow PV) = \frac{\tau_B}{8\pi} \frac{|P_c|}{m_B^2} |\mathcal{A}(B \rightarrow PV)|^2, \quad (16)$$

where  $\tau_B$  is the B meson lifetimes, and  $|P_c|$  is the absolute values of final-state hadrons' momentum in the B rest frame and written as

$$|P_c| = \frac{\sqrt{[m_B^2 - (m_P + m_V)^2][m_B^2 - (m_P - m_V)^2]}}{2m_B}. \quad (17)$$

For the CP-conjugated decay modes, the branching ratios can be obtained by replacing CKM factors with their complex conjugate in the expressions of decay amplitudes. Using the decay amplitudes as given in Refs. [8, 13] and the coefficients  $a_i$  in Eq.(8) or  $\alpha_i$  in Eq.(11), it is straightforward to calculate the CP-averaged branching ratios of those thirty nine  $B \rightarrow PV$  decay modes in the SM and mSUGRA model.

From Eqs.(8-11), we can find that the potential SUSY contributions are mainly embodied in  $\alpha_4^p(M_1 M_2)$  and  $\alpha_{4,ew}^p(M_1 M_2)$ . Therefore, one naturally expect a large new physics corrections to those penguin dominated B meson decays.

## A. Numerical results

In Table II and III, we show the theoretical predictions for the CP-averaged branching ratios for  $B \rightarrow PV$  decays in both the SM and mSUGRA model, assuming  $\mu = m_b/2, m_b$  and  $2m_b$ , respectively. And in the SM we give both  $Br^{f+a}$  and  $Br^f$ , the SM predictions for the branching ratios with or without the inclusion of annihilation contributions, respectively. In the mSUGRA model, we consider both case B and case C and only give  $Br^f$  so that we can compare the relative size of the new physics contribution with the annihilation contribution for each considered decay channel. From the numerical results, one can see that the SUSY corrections to the  $b \rightarrow s$  transition processes are generally larger than those to the  $b \rightarrow d$  processes because of the CKM factor suppression ( $|V_{tb}V_{td}^*| \sim 10^{-2}$ ) in  $b \rightarrow d$  penguin transition.

We classify the thirty nine  $B \rightarrow PV$  channels into  $b \rightarrow d$  and  $b \rightarrow s$  processes. For  $b \rightarrow d$  processes, we have the following remarks

- The  $\bar{B}^0 \rightarrow \pi^\pm \rho^\mp$  and  $B^- \rightarrow \pi^0 \rho^-, \pi^- \rho^0, \pi^- \omega, \eta^{(\prime)} \rho^-$  decays.

These channels are tree-dominated decay modes and depend on the large coefficient  $\alpha_1$ . The SUSY corrections to these decays are very small and can be neglected safely in all the parameter space.

- The decays  $\bar{B}^0 \rightarrow \pi^0 \rho^0, \pi^0 \omega, \eta^{(\prime)} \rho^0, \eta^{(\prime)} \omega$ .

These channels have small branching ratios. The reason for this is twofold. On the one hand, the tree contributions of these channels are involved in the coefficient  $\alpha_2 \sim 0.2$ , which is far smaller than the large coefficient  $\alpha_1 \sim 1$ . The penguin contributions,

TABLE II: Numerical predictions in the SM and mSUGRA model for CP-averaged branching ratios ( in units of  $10^{-6}$ ) for  $b \rightarrow d$  transition processes of  $B \rightarrow PV$  decays, where  $Br^{f+a}$  and  $Br^f$  denotes the branching ratios with and without the annihilation contributions respectively. For Case B and C, the branching ratios without annihilation contributions are given.

| $B \rightarrow PV$<br>( $b \rightarrow d$ ) | $\mu = m_b/2$ |            |        |       | $\mu = m_b$ |            |        |       | $\mu = 2m_b$ |            |        |       |
|---------------------------------------------|---------------|------------|--------|-------|-------------|------------|--------|-------|--------------|------------|--------|-------|
|                                             | SM            |            | mSUGRA |       | SM          |            | mSUGRA |       | SM           |            | mSUGRA |       |
|                                             | $Br^f$        | $Br^{f+a}$ | (B)    | (C)   | $Br^f$      | $Br^{f+a}$ | (B)    | (C)   | $Br^f$       | $Br^{f+a}$ | (B)    | (C)   |
| $B^- \rightarrow \pi^- \rho^0$              | 11.2          | 11.2       | 11.2   | 11.2  | 11.5        | 11.4       | 11.5   | 11.5  | 11.8         | 11.8       | 11.8   | 11.8  |
| $B^- \rightarrow \pi^0 \rho^-$              | 14.8          | 14.9       | 14.9   | 14.8  | 14.9        | 15.0       | 15.0   | 14.9  | 15.1         | 15.2       | 15.2   | 15.1  |
| $\bar{B}^0 \rightarrow \pi^+ \rho^-$        | 21.2          | 22.3       | 21.5   | 21.2  | 21.2        | 22.1       | 21.4   | 22.2  | 20.9         | 21.7       | 21.2   | 20.9  |
| $\bar{B}^0 \rightarrow \pi^- \rho^+$        | 14.3          | 15.1       | 14.4   | 14.3  | 14.3        | 14.9       | 14.3   | 14.3  | 14.1         | 14.7       | 14.2   | 14.1  |
| $B^- \rightarrow \pi^- \omega$              | 9.09          | 8.70       | 9.24   | 9.09  | 9.25        | 8.98       | 9.38   | 9.25  | 9.48         | 9.29       | 9.59   | 9.48  |
| $B^- \rightarrow \eta \rho^-$               | 6.50          | 6.19       | 6.61   | 6.50  | 6.55        | 6.35       | 6.64   | 6.55  | 6.67         | 6.52       | 6.75   | 6.67  |
| $B^- \rightarrow \eta' \rho^-$              | 4.60          | 4.39       | 4.67   | 4.60  | 4.66        | 4.51       | 4.71   | 4.66  | 4.78         | 4.67       | 4.82   | 4.78  |
| $\bar{B}^0 \rightarrow \pi^0 \rho^0$        | 0.538         | 0.417      | 0.532  | 0.538 | 0.524       | 0.419      | 0.512  | 0.523 | 0.602        | 0.502      | 0.585  | 0.601 |
| $\bar{B}^0 \rightarrow \pi^0 \omega$        | 0.019         | 0.013      | 0.043  | 0.019 | 0.014       | 0.007      | 0.032  | 0.014 | 0.012        | 0.004      | 0.025  | 0.012 |
| $\bar{B}^0 \rightarrow \eta \rho^0$         | 0.004         | 0.021      | 0.010  | 0.004 | 0.003       | 0.016      | 0.006  | 0.003 | 0.003        | 0.014      | 0.004  | 0.003 |
| $\bar{B}^0 \rightarrow \eta' \rho^0$        | 0.035         | 0.066      | 0.033  | 0.035 | 0.033       | 0.058      | 0.029  | 0.033 | 0.034        | 0.055      | 0.029  | 0.034 |
| $\bar{B}^0 \rightarrow \eta \omega$         | 0.278         | 0.351      | 0.295  | 0.278 | 0.249       | 0.308      | 0.262  | 0.249 | 0.269        | 0.323      | 0.279  | 0.269 |
| $\bar{B}^0 \rightarrow \eta' \omega$        | 0.274         | 0.337      | 0.283  | 0.274 | 0.253       | 0.305      | 0.259  | 0.253 | 0.276        | 0.323      | 0.281  | 0.276 |
| $B^- \rightarrow \pi^- \phi$                | 0.008         | —          | 0.008  | 0.008 | 0.006       | —          | 0.006  | 0.006 | 0.005        | —          | 0.005  | 0.005 |
| $\bar{B}^0 \rightarrow \pi^0 \phi$          | 0.003         | —          | 0.003  | 0.003 | 0.002       | —          | 0.002  | 0.002 | 0.002        | —          | 0.002  | 0.002 |
| $\bar{B}^0 \rightarrow \eta \phi$           | 0.002         | 0.001      | 0.002  | 0.002 | 0.001       | 0.001      | 0.001  | 0.001 | 0.001        | 0.0008     | 0.001  | 0.001 |
| $\bar{B}^0 \rightarrow \eta' \phi$          | 0.002         | 0.003      | 0.002  | 0.002 | 0.001       | 0.002      | 0.001  | 0.001 | 0.001        | 0.0011     | 0.001  | 0.001 |
| $B^- \rightarrow K^- K^{*0}$                | 0.12          | 0.17       | 0.31   | 0.12  | 0.11        | 0.15       | 0.28   | 0.11  | 0.10         | 0.12       | 0.24   | 0.10  |
| $\bar{B}^0 \rightarrow \bar{K}^0 K^{*0}$    | 0.11          | 0.14       | 0.29   | 0.11  | 0.10        | 0.13       | 0.26   | 0.11  | 0.09         | 0.11       | 0.22   | 0.10  |
| $B^- \rightarrow K^0 K^{*-}$                | 0.10          | 0.16       | 0.03   | 0.10  | 0.11        | 0.16       | 0.04   | 0.11  | 0.13         | 0.17       | 0.07   | 0.13  |
| $\bar{B}^0 \rightarrow K^0 \bar{K}^{*0}$    | 0.09          | 0.15       | 0.02   | 0.09  | 0.10        | 0.15       | 0.04   | 0.10  | 0.12         | 0.16       | 0.06   | 0.12  |
| $\bar{B}^0 \rightarrow K^+ K^{*-}$          | —             | 0.02       | —      | —     | —           | 0.01       | —      | —     | —            | 0.01       | —      | —     |
| $\bar{B}^0 \rightarrow K^- K^{*+}$          | —             | 0.02       | —      | —     | —           | 0.01       | —      | —     | —            | 0.01       | —      | —     |

on the other hand, are strongly suppressed by the CKM factor  $|V_{tb}V_{td}^*| \sim 10^{-2}$ . From Table II, we can see that the SUSY corrections are always smaller than the annihilation contributions, and thus can be easily masked by it.

- The decays  $\bar{B}^0 \rightarrow \pi^0 \phi, \eta^{(\prime)} \phi$  and  $B^- \rightarrow \pi^- \phi$ .

This kind of channels have both penguin and weak annihilation contributions. But the penguin contributions come from the small coefficients  $\alpha_3^P$  and  $\alpha_{3,ew}^P$ . Therefore weak annihilation contributions are dominant for  $\bar{B}^0 \rightarrow \eta^{(\prime)} \phi$ . The branching ratios of these decay are at the  $\mathcal{O}(10^{-9})$  level, and the SUSY corrections in all parameter

TABLE III: Numerical predictions in the SM and mSUGRA model for CP-averaged branching ratios (in units of  $10^{-6}$ ) for  $b \rightarrow s$  transition process of  $B \rightarrow PV$  decays, where  $Br^{f+a}$  and  $Br^f$  denotes the branching ratios with and without the annihilation contributions respectively. For Case B and C, the branching ratios without annihilation contributions are given.

| $B \rightarrow PV$<br>( $b \rightarrow s$ ) | $\mu = m_b/2$ |            |        |      | $\mu = m_b$ |            |        |      | $\mu = 2m_b$ |            |        |      |
|---------------------------------------------|---------------|------------|--------|------|-------------|------------|--------|------|--------------|------------|--------|------|
|                                             | SM            |            | mSUGRA |      | SM          |            | mSUGRA |      | SM           |            | mSUGRA |      |
|                                             | $Br^f$        | $Br^{f+a}$ | (B)    | (C)  | $Br^f$      | $Br^{f+a}$ | (B)    | (C)  | $Br^f$       | $Br^{f+a}$ | (B)    | (C)  |
| $B^- \rightarrow \pi^- K^{*0}$              | 2.19          | 3.17       | 5.85   | 2.21 | 2.08        | 2.83       | 5.26   | 2.10 | 1.82         | 2.39       | 4.57   | 1.83 |
| $B^- \rightarrow \pi^0 K^{*-}$              | 2.00          | 2.37       | 4.15   | 2.02 | 1.94        | 2.23       | 3.85   | 1.96 | 1.81         | 2.03       | 3.50   | 1.82 |
| $\bar{B}^0 \rightarrow \pi^0 \bar{K}^{*0}$  | 0.33          | 0.49       | 1.45   | 0.33 | 0.30        | 0.42       | 1.24   | 0.30 | 0.24         | 0.33       | 1.03   | 0.24 |
| $\bar{B}^0 \rightarrow \pi^+ K^{*-}$        | 1.68          | 2.27       | 4.38   | 1.70 | 1.62        | 2.07       | 3.99   | 1.64 | 1.49         | 1.82       | 3.55   | 1.50 |
| $B^- \rightarrow K^- \phi$                  | 2.73          | 4.08       | 6.06   | 2.75 | 2.46        | 3.47       | 5.31   | 2.47 | 2.04         | 2.79       | 4.49   | 2.05 |
| $\bar{B}^0 \rightarrow \bar{K}^0 \phi$      | 2.53          | 3.66       | 5.60   | 2.55 | 2.27        | 3.12       | 4.90   | 2.28 | 1.89         | 2.52       | 4.15   | 1.90 |
| $B^- \rightarrow K^- \rho^0$                | 1.24          | 1.70       | 0.72   | 1.23 | 1.39        | 1.77       | 0.87   | 1.38 | 1.66         | 2.01       | 1.12   | 1.65 |
| $B^- \rightarrow \bar{K}^0 \rho^-$          | 1.92          | 3.08       | 0.55   | 1.91 | 2.14        | 3.07       | 0.89   | 2.13 | 2.58         | 3.29       | 1.39   | 2.57 |
| $\bar{B}^0 \rightarrow K^- \rho^+$          | 4.05          | 5.61       | 2.11   | 4.02 | 4.38        | 5.64       | 2.64   | 4.35 | 4.91         | 5.98       | 3.32   | 4.88 |
| $\bar{B}^0 \rightarrow \bar{K}^0 \rho^0$    | 2.22          | 3.10       | 1.11   | 2.20 | 2.32        | 3.02       | 1.37   | 2.31 | 2.52         | 3.10       | 1.69   | 2.51 |
| $B^- \rightarrow K^- \omega$                | 2.43          | 3.14       | 1.43   | 2.41 | 2.33        | 2.87       | 1.51   | 2.32 | 2.51         | 2.95       | 1.76   | 2.50 |
| $\bar{B}^0 \rightarrow \bar{K}^0 \omega$    | 1.09          | 1.66       | 0.45   | 1.09 | 0.99        | 1.41       | 0.46   | 0.98 | 1.11         | 1.46       | 0.62   | 1.10 |
| $B^- \rightarrow \eta K^{*-}$               | 4.31          | 5.64       | 4.68   | 4.32 | 4.64        | 5.72       | 5.26   | 4.65 | 5.18         | 6.08       | 6.06   | 5.20 |
| $\bar{B}^0 \rightarrow \eta \bar{K}^{*0}$   | 4.58          | 5.98       | 4.86   | 4.58 | 4.94        | 6.07       | 5.45   | 4.94 | 5.46         | 6.40       | 6.20   | 5.46 |
| $B^- \rightarrow \eta' K^{*-}$              | 1.86          | 2.71       | 0.93   | 1.84 | 2.13        | 2.95       | 0.83   | 2.11 | 2.51         | 3.25       | 1.12   | 2.49 |
| $\bar{B}^0 \rightarrow \eta' \bar{K}^{*0}$  | 1.21          | 1.99       | 0.61   | 1.20 | 1.40        | 2.17       | 0.43   | 1.38 | 1.72         | 2.42       | 0.65   | 1.71 |

space can hardly affect them.

- The decays  $\bar{B}^0 \rightarrow \bar{K}^0 K^{*0}$  and  $B^- \rightarrow K^- K^{*0}$ .

These channels are penguin dominant decays. In their amplitudes, the dominant term is proportional to  $\alpha_4^P(P, V)$  and  $\alpha_{4,ew}^P(P, V)$ . The SUSY corrections therefore can increase their branching ratios significantly in some parameter space, such as in case B where the SUSY contributions can provide a 130% enhancement and are far larger than the annihilation contributions. But in case C where  $C_{7\gamma}(m_b)$  is SM-like, the SUSY contributions are negligibly small.

- The decays  $\bar{B}^0 \rightarrow K^0 \bar{K}^{*0}$  and  $B^- \rightarrow K^0 K^{*-}$ .

Different from the  $\bar{B}^0 \rightarrow \bar{K}^0 K^{*0}$  and  $B^- \rightarrow K^- K^{*0}$  decays, the dominant terms here are proportional to  $\alpha_4^P(V, P)$  and  $\alpha_{4,ew}^P(V, P)$ . The SUSY corrections interfere destructively with their SM counterparts and will decrease the branching ratios by about 50% in case B. For case C, the SUSY contributions are still very small.

- The decays  $\bar{B}^0 \rightarrow K^+ K^{*-}, K^- K^{*+}$ .

These two channels have weak annihilation contributions only. Therefore in the mSUGRA model their branching ratios can hardly be affected.

For  $b \rightarrow s$  transition processes, the tree contribution is suppressed by CKM factors, the penguin contributions therefore play the major role. These decays can be classified into three groups. And our remarks are

- $B \rightarrow \pi K^*, K\phi$  decays.

These decays are penguin dominant decays and both the annihilation contributions and the SUSY contributions can give enhancements to their branching ratios. But for case C the SUSY contributions are smaller than the annihilation contributions and can be masked easily. Only in case B where the enhancements can reach as large as 100%  $\sim$  260% for  $B \rightarrow \pi K^*$  decay and about 100% for  $B \rightarrow K\phi$  decay.

- $B \rightarrow K\rho, K\omega$  decays.

In case B the branching ratios of these decays will be decreased by 30%  $\sim$  60% after the inclusion of SUSY corrections and theoretically we can isolate the SUSY contributions from the annihilation contributions for which tend to increase the branching ratios greatly. In case C, however, the SUSY contributions are small, while the annihilation contributions are relatively important for explaining the current large measured data.

- $B \rightarrow K^*\eta^{(\prime)}$  decays.

For  $B \rightarrow K^*\eta$  decay, their amplitudes strongly depend on  $\alpha_4^P(P, V)$  and  $\alpha_{4,ew}^P(P, V)$ . Although the inclusion of SUSY corrections will increase their branching ratios, the SUSY contributions will also be masked by large annihilation contributions. For  $B \rightarrow K^*\eta'$  decay, however, their amplitudes mainly depend on  $\alpha_4^P(V, P)$  and  $\alpha_{4,ew}^P(V, P)$ , the SUSY corrections will trend to decrease their branching ratios in both cases and can be separated from the annihilation contributions which can contribute a 40%  $\sim$  60% enhancement to the branching ratios.

From above discussions, one can see that the SUSY contributions in case-C (preferred by the measured branching ratio of  $B \rightarrow X_s l^+ l^-$  decay [37]) are always negligibly small.

## B. The data and phenomenological analysis

Among the thirty nine  $B \rightarrow PV$  decay modes considered here, eighteen of them have been measured experimentally. The latest individual measurements as reported by different groups and the new world average for the branching ratios can be found in the HFAG (Heavy Flavor Averaging Group) homepage [42]. In this subsection we will make a phenomenological discussion for those eighteen measured decay channels.

### 1. $B \rightarrow \pi\rho$ and $B \rightarrow \pi\omega$

Among the  $B \rightarrow \pi\rho$  and  $\pi\omega$  decays, four of them have been well measured, and the experimental upper limits are available for the remaining  $B \rightarrow \pi^0\rho^0$  and  $\pi^0\omega$  decay modes.

The data and the theoretical predictions for the four measured decay modes (in units of  $10^{-6}$ ) in the SM and mSUGRA model (both Case B and Case C) are

$$Br(B^0 \rightarrow \pi^\pm \rho^\mp) = \begin{cases} 24.0 \pm 2.5, & \text{Data,} \\ 37.0_{-4.6}^{+5.4}(A_0^{B \rightarrow \rho}) \begin{smallmatrix} +9.0 \\ -7.4 \end{smallmatrix} (F_1^{B \rightarrow \pi}) \begin{smallmatrix} +3.1 \\ -2.1 \end{smallmatrix} (\chi_A) \pm 1.7(\gamma), & \text{SM,} \\ 37.3_{-4.6}^{+5.4}(A_0^{B \rightarrow \rho}) \begin{smallmatrix} +9.1 \\ -7.5 \end{smallmatrix} (F_1^{B \rightarrow \pi}) \begin{smallmatrix} +3.1 \\ -2.1 \end{smallmatrix} (\chi_A) \begin{smallmatrix} +1.9 \\ -2.0 \end{smallmatrix} (\gamma), & \text{Case - B,} \\ 37.0_{-4.5}^{+5.4}(A_0^{B \rightarrow \rho}) \begin{smallmatrix} +9.9 \\ -7.5 \end{smallmatrix} (F_1^{B \rightarrow \pi}) \begin{smallmatrix} +3.0 \\ -2.1 \end{smallmatrix} (\chi_A) \begin{smallmatrix} +1.7 \\ -1.8 \end{smallmatrix} (\gamma), & \text{Case - C,} \end{cases} \quad (18)$$

$$Br(B^- \rightarrow \pi^- \rho^0) = \begin{cases} 8.7_{-1.1}^{+1.0}, & \text{Data,} \\ 11.4_{-3.0}^{+3.4}(A_0^{B \rightarrow \rho}) \begin{smallmatrix} +0.9 \\ -0.7 \end{smallmatrix} (\gamma), & \text{SM,} \\ 11.4_{-3.0}^{+3.4}(A_0^{B \rightarrow \rho}) \begin{smallmatrix} +1.0 \\ -0.8 \end{smallmatrix} (\gamma), & \text{Case - B,} \\ 11.4_{-2.9}^{+3.5}(A_0^{B \rightarrow \rho}) \begin{smallmatrix} +0.9 \\ -0.6 \end{smallmatrix} (\gamma), & \text{Case - C,} \end{cases} \quad (19)$$

$$Br(B^- \rightarrow \pi^0 \rho^-) = \begin{cases} 10.8_{-1.5}^{+1.4}, & \text{Data,} \\ 15.0_{-4.6}^{+5.4}(F_1^{B \rightarrow \pi}) \begin{smallmatrix} +0.5 \\ -0.2 \end{smallmatrix} (\chi_A) \begin{smallmatrix} +0.9 \\ -1.1 \end{smallmatrix} (\gamma), & \text{SM,} \\ 15.1_{-4.6}^{+5.4}(F_1^{B \rightarrow \pi}) \begin{smallmatrix} +0.5 \\ -0.2 \end{smallmatrix} (\chi_A) \begin{smallmatrix} +1.2 \\ -1.0 \end{smallmatrix} (\gamma), & \text{Case - B,} \\ 15.0_{-4.5}^{+5.4}(F_1^{B \rightarrow \pi}) \begin{smallmatrix} +0.5 \\ -0.2 \end{smallmatrix} (\chi_A) \begin{smallmatrix} +0.9 \\ -1.1 \end{smallmatrix} (\gamma), & \text{Case - C,} \end{cases} \quad (20)$$

$$Br(B^- \rightarrow \pi^- \omega) = \begin{cases} 6.6 \pm 0.6, & \text{Data,} \\ 9.0_{-2.2}^{+2.5}(A_0^{B \rightarrow \omega}) \begin{smallmatrix} +0.4 \\ -0.5 \end{smallmatrix} (\chi_A), & \text{SM,} \\ 9.1_{-2.2}^{+2.5}(A_0^{B \rightarrow \omega}) \begin{smallmatrix} +0.4 \\ -0.5 \end{smallmatrix} (\chi_A), & \text{Case - B,} \\ 9.0_{-2.2}^{+2.5}(A_0^{B \rightarrow \omega}) \begin{smallmatrix} +0.4 \\ -0.5 \end{smallmatrix} (\chi_A), & \text{Case - C,} \end{cases} \quad (21)$$

where the major errors are induced by the uncertainties of the following input parameters:  $F_1^{B \rightarrow \pi} = 0.28 \pm 0.05$ ,  $A_0^{B \rightarrow \rho} = 0.37 \pm 0.06$ ,  $A_0^{B \rightarrow \omega} = 0.33 \pm 0.05$  and  $\gamma = 57.8^\circ \pm 20^\circ$ . Throughout this paper we take the central values and the ranges of these input parameters specified here as the default values, unless explicitly stated otherwise.

We also set  $\rho_A = 0$  as the default input value [11] in numerical calculations, and scan over  $\rho_A \in [0, 1]$  and  $\phi_A \in [-180^\circ, 180^\circ]$  to estimate the theoretical error induced by the uncertainty of annihilation contribution.

For the convenience of analysis, in Fig. 1 we show the  $\gamma$  dependence of the theoretical predictions<sup>3</sup> for the branching ratios of the three  $B \rightarrow \pi \rho$  and  $B^- \rightarrow \pi^- \omega$  decays respectively and the experimental data are also marked.

From the numerical results as given in Eqs.(18-21) and Fig. 1, one can see that

- For these tree-dominated decay modes, the SUSY corrections in the mSUGRA model are always very small for  $\gamma \sim 60^\circ$ .
- As to the theoretical errors, generally the uncertainties of the form factors and the annihilation contribution are the dominant sources. For  $B^0 \rightarrow \pi^\pm \rho^\mp$ , the annihilation contribution which has been parameterized by  $\chi_A$  also give large uncertainty. For  $B^- \rightarrow \pi^- \rho^0$ , however, the uncertainty of the annihilation contribution is small and has been ignored here.

<sup>3</sup> The central values of all input parameters except for the CKM angle  $\gamma$  are used in this and other similar figures. The theoretical uncertainties are not shown in all such kinds of figures.

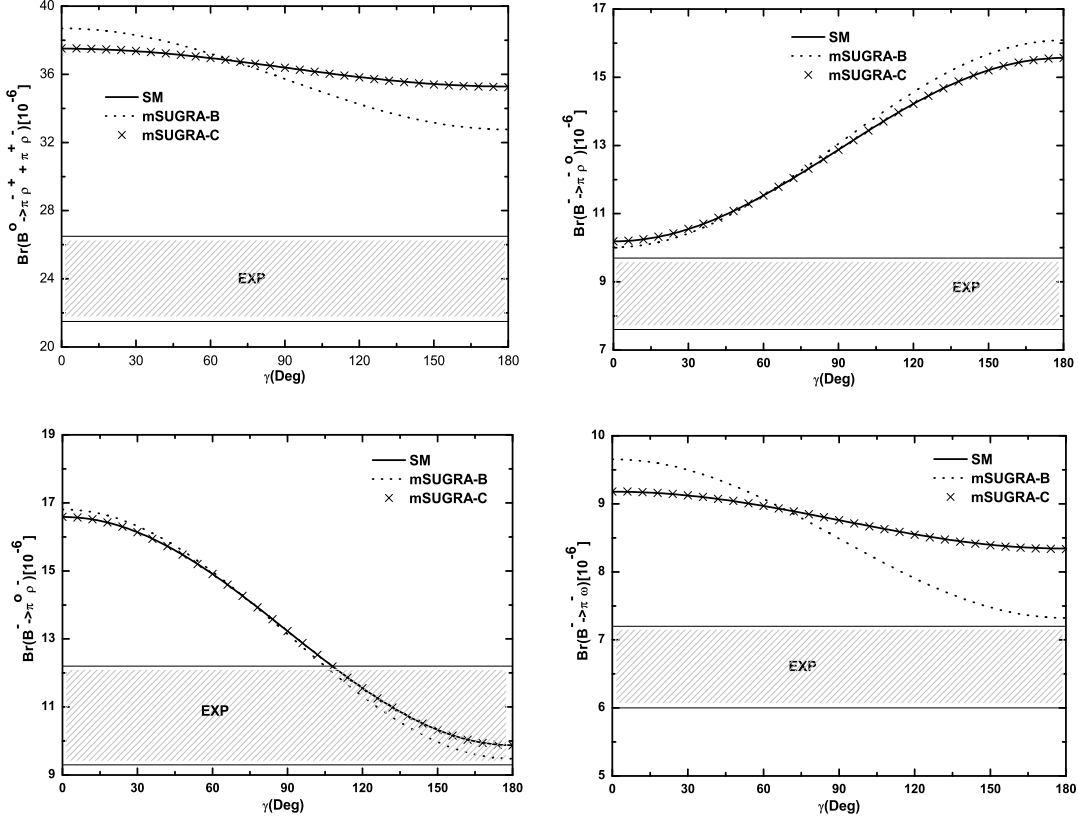


FIG. 1: The  $\gamma$  dependence of the branching ratios of  $B \rightarrow \pi\rho$  and  $B^- \rightarrow \pi^-\omega$  decays in the SM and mSUGRA model. The solid, dots lines and the scatter of prong show the central values of the SM prediction and the mSUGRA ones in both case B and case C, respectively. The horizontal back-slashd gray bands show the data.

- The theoretical predictions for the branching ratios in both the SM and mSUGRA model are all consistent with the data within one standard deviation since the theoretical errors are still large.

## 2. $B \rightarrow \pi K^*$ , $B \rightarrow K\phi$

Like  $B \rightarrow \pi K$ , the four  $B \rightarrow \pi K^*$  decays are penguin dominated decay modes and therefore sensitive to the new physics contributions. The CP-averaged branching ratios of the four  $B \rightarrow \pi K^*$  decays have been measured experimentally and the data are much larger than the SM predictions. In the mSUGRA model, the new penguin diagrams may contribute effectively to these decays. The data and the numerical results (in units of

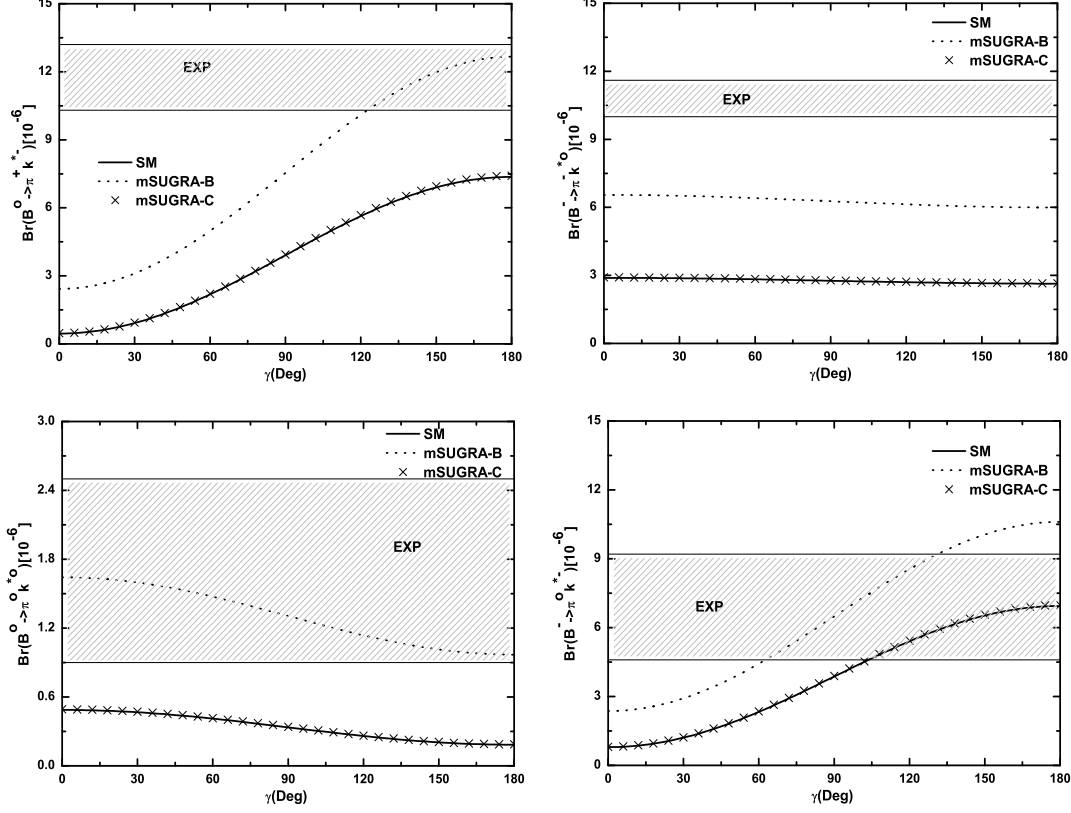


FIG. 2: The same as Fig.1 but for  $B \rightarrow \pi K^*$  decays.

$10^{-6}$ ) are

$$Br(\bar{B}^0 \rightarrow \pi^+ K^{*-}) = \begin{cases} 11.7_{-1.4}^{+1.5}, & \text{Data,} \\ 2.1_{-0.3}^{+0.2}(\mu) + 0.8(F_1^{B \rightarrow \pi}) + 4.4(\chi_A) + 1.1(\gamma), & \text{SM,} \\ 4.8 \pm 0.7(\mu) + 1.8(F_1^{B \rightarrow \pi}) + 6.5(\chi_A) + 1.7(\gamma), & \text{Case - B,} \\ 2.1_{-0.3}^{+0.2}(\mu) + 0.8(F_1^{B \rightarrow \pi}) + 4.4(\chi_A) + 1.1(\gamma), & \text{Case - C,} \end{cases} \quad (22)$$

$$Br(B^- \rightarrow \pi^- \bar{K}^{*0}) = \begin{cases} 10.8 \pm 0.8, & \text{Data,} \\ 2.8_{-0.4}^{+0.3}(\mu) + 1.1(F_1^{B \rightarrow \pi}) + 6.1(\chi_A), & \text{SM,} \\ 6.4 \pm 1.0(\mu) + 2.5(F_1^{B \rightarrow \pi}) + 8.3(\chi_A), & \text{Case - B,} \\ 2.9_{-0.5}^{+0.3}(\mu) + 1.1(F_1^{B \rightarrow \pi}) + 6.1(\chi_A), & \text{Case - C,} \end{cases} \quad (23)$$



$$Br(\bar{B}^0 \rightarrow \pi^0 \bar{K}^{*0}) = \begin{cases} 1.7 \pm 0.8, & \text{Data,} \\ 0.4^{+0.3}_{-0.2}(F_1^{B \rightarrow \pi}) \pm 0.1(A_0^{B \rightarrow K^*})^{+1.4}_{-0.3}(\chi_A), & \text{SM,} \\ 1.5^{+0.9}_{-0.7}(F_1^{B \rightarrow \pi}) \pm 0.2(A_0^{B \rightarrow K^*})^{+2.2}_{-0.7}(\chi_A), & \text{Case - B,} \\ 0.4^{+0.3}_{-0.2}(F_1^{B \rightarrow \pi}) \pm 0.1(A_0^{B \rightarrow K^*})^{+1.4}_{-0.3}(\chi_A), & \text{Case - C,} \end{cases} \quad (24)$$

$$Br(B^- \rightarrow \pi^0 \bar{K}^{*-}) = \begin{cases} 6.9 \pm 2.3, & \text{Data,} \\ 2.2^{+0.6}_{-0.5}(F_1^{B \rightarrow \pi})^{+0.3}_{-0.2}(A_0^{B \rightarrow K^*})^{+2.5}_{-0.8}(\chi_A)^{+1.0}_{-0.8}(\gamma), & \text{SM,} \\ 4.3^{+1.2}_{-1.1}(F_1^{B \rightarrow \pi})^{+0.4}_{-0.3}(A_0^{B \rightarrow K^*})^{+3.4}_{-1.3}(\chi_A)^{+1.3}_{-0.1}(\gamma), & \text{Case - B,} \\ 2.3^{+0.6}_{-0.5}(F_1^{B \rightarrow \pi})^{+0.3}_{-0.2}(A_0^{B \rightarrow K^*})^{+2.5}_{-0.8}(\chi_A)^{+1.0}_{-0.8}(\gamma), & \text{Case - C,} \end{cases} \quad (25)$$

where the renormalization scale  $\mu$  varies from  $m_b/2$  to  $2m_b$ , and the second error in Eq.(24) and (25) is induced by the uncertainty of the form factor  $A_0^{B \rightarrow K^*}$ ,  $A_0^{B \rightarrow K^*} = 0.45 \pm 0.07$ .

Fig. 2 shows the  $\gamma$  dependence of the branching ratios for the measured  $B \rightarrow \pi K^*$  decays in both the SM and the mSUGRA model. From this figure and Eqs.(22-25), one can see that

- The central values of the SM predictions for the branching ratios are only about 20 to 30 percent of the measured values. The SUSY contributions are also very small in the parameter space where  $C_{7\gamma}(m_b)$  is SM-like. But for the case B, the SUSY contributions are large and can provide a factor of two enhancements to these penguin-dominated decays. After the inclusion of the large SUSY contributions, the mSUGRA predictions for  $B \rightarrow \pi^- \bar{K}^{*0}$ ,  $\pi^0 K^{*-}$  and  $\pi^0 K^{*0}$  become consistent with the data within one standard deviation.
- For all the four  $B \rightarrow \pi K^*$  decays, the dominant error is induced by the uncertainty of the annihilation contribution, it is large and may mask the large SUSY contributions in Case B.
- After the inclusion of the large theoretical errors, the theoretical predictions for the branching ratios of  $B \rightarrow \pi^- \bar{K}^{*0}$ ,  $\pi^0 K^{*-}$  and  $\pi^0 K^{*0}$  in both models can be consistent with the corresponding data within one standard deviation. But for  $\bar{B}^0 \rightarrow \pi^+ K^{*-}$  decay, only when we include the large SUSY contribution in Case B as well can the theoretical value match with the data within one standard deviation.

Like  $B \rightarrow \pi K^*$ , the SUSY contributions to  $B \rightarrow K \phi$  in case B are large and can provide about 100% enhancement. From Fig. 3, one can see that the mSUGRA predictions in case B can become consistent with the data within one standard deviation. The data, the central values and the major errors of the branching ratios (in units of  $10^{-6}$ ) in the SM and mSUGRA model are

$$Br(\bar{B}^0 \rightarrow \bar{K}^0 \phi) = \begin{cases} 8.3^{+1.2}_{-1.0}, & \text{Data,} \\ 3.1^{+0.5}_{-0.6}(\mu)^{+1.1}_{-0.9}(F_1^{B \rightarrow K})^{+8.0}_{-2.2}(\chi_A), & \text{SM,} \\ 6.1 \pm 1.1(\mu)^{+2.1}_{-1.8}(F_1^{B \rightarrow K})^{+10.2}_{-3.3}(\chi_A), & \text{Case - B,} \\ 3.1^{+0.5}_{-0.6}(\mu)^{+1.1}_{-0.9}(F_1^{B \rightarrow K})^{+8.0}_{-2.2}(\chi_A), & \text{Case - C,} \end{cases} \quad (26)$$

$$Br(B^- \rightarrow K^- \phi) = \begin{cases} 9.0 \pm 0.7, & \text{Data,} \\ 3.5^{+0.6}_{-0.7}(\mu)^{+1.2}_{-1.0}(F_1^{B \rightarrow K})^{+9.0}_{-2.4}(\chi_A), & \text{SM,} \\ 6.8^{+1.3}_{-1.2}(\mu)^{+2.3}_{-1.9}(F_1^{B \rightarrow K})^{+11.5}_{-3.7}(\chi_A), & \text{Case - B,} \\ 3.5^{+0.6}_{-0.7}(\mu)^{+1.2}_{-1.0}(F_1^{B \rightarrow K})^{+9.0}_{-2.4}(\chi_A), & \text{Case - C.} \end{cases} \quad (27)$$

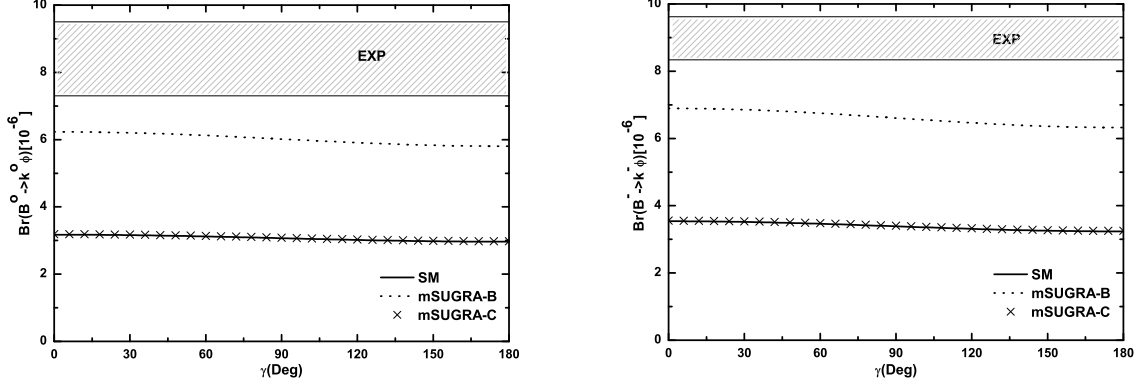


FIG. 3: The same as Fig.1 but for  $B \rightarrow K\phi$  decays.

From these numerical results, one can see that (a) the central values of the SM predictions are only about one third of the measured values. But the mSUGRA predictions in case B can become consistent with the data within one standard deviation. (b) Similar to the  $B \rightarrow \pi K^*$  decays, the dominant error here also comes from the uncertainty of the annihilation contribution and the form factor  $F_1^{B \rightarrow K}$ . The error induced by  $\chi_A$  are very large and even mask the large SUSY contributions in Case B.

### 3. $B \rightarrow K\rho$ , $B \rightarrow K\omega$

Among the four  $B \rightarrow K\rho$  decays, three of them have been well measured experimentally. The data, the theoretical predictions and the major errors (in units of  $10^{-6}$ ) are

$$Br(\bar{B}^0 \rightarrow K^- \rho^+) = \begin{cases} 9.9^{+1.6}_{-1.5}, & \text{Data,} \\ 5.6^{+1.7}_{-1.5}(A_0^{B \rightarrow \rho})^{+0.9}_{-1.1}(\gamma)^{+3.8}_{-2.0}(\bar{m}_s)^{+8.1}_{-2.6}(\chi_A), & \text{SM,} \\ 3.6^{+1.1}_{-0.9}(A_0^{B \rightarrow \rho})^{+0.6}_{-0.7}(\gamma)^{+3.3}_{-1.5}(\bar{m}_s)^{+6.6}_{-1.9}(\chi_A), & \text{Case - B,} \\ 5.6^{+1.7}_{-1.5}(A_0^{B \rightarrow \rho})^{+0.9}_{-1.1}(\gamma)^{+3.8}_{-1.9}(\bar{m}_s)^{+8.1}_{-2.6}(\chi_A), & \text{Case - C,} \end{cases} \quad (28)$$

$$Br(B^- \rightarrow K^- \rho^0) = \begin{cases} 4.23^{+0.56}_{-0.57}, & \text{Data,} \\ 1.8 \pm 0.2(F_1^{B \rightarrow K})^{+0.7}_{-0.6}(A_0^{B \rightarrow \rho})^{+1.5}_{-0.7}(\bar{m}_s)^{+3.1}_{-0.8}(\chi_A), & \text{SM,} \\ 1.1 \pm 0.1(F_1^{B \rightarrow K}) \pm 0.4(A_0^{B \rightarrow \rho})^{+1.2}_{-0.4}(\bar{m}_s)^{+2.3}_{-0.4}(\chi_A), & \text{Case - B,} \\ 1.8 \pm 0.2(F_1^{B \rightarrow K})^{+0.7}_{-0.6}(A_0^{B \rightarrow \rho})^{+1.4}_{-0.7}(\bar{m}_s)^{+3.0}_{-0.8}(\chi_A), & \text{Case - C,} \end{cases} \quad (29)$$

$$Br(\bar{B}^0 \rightarrow \bar{K}^0 \rho^0) = \begin{cases} 5.1 \pm 1.6, & \text{Data,} \\ 3.0 \pm 0.3(F_1^{B \rightarrow K}) \pm 0.5(A_0^{B \rightarrow \rho})^{+1.9}_{-1.1}(\bar{m}_s)^{+4.4}_{-1.5}(\chi_A), & \text{SM,} \\ 1.9 \pm 0.3(F_1^{B \rightarrow K}) \pm 0.2(A_0^{B \rightarrow \rho})^{+1.7}_{-0.9}(\bar{m}_s)^{+3.7}_{-1.1}(\chi_A), & \text{Case - B,} \\ 3.0 \pm 0.3(F_1^{B \rightarrow K}) \pm 0.5(A_0^{B \rightarrow \rho})^{+1.9}_{-1.0}(\bar{m}_s)^{+4.3}_{-1.5}(\chi_A), & \text{Case - C.} \end{cases} \quad (30)$$

Here the new dominant error source is the uncertainty of the mass  $\bar{m}_s$ ,  $85 \text{ MeV} \leq \bar{m}_s \leq 125 \text{ MeV}$ . In Fig. 4, we show the  $\gamma$  dependence of the branching ratios for the three measured

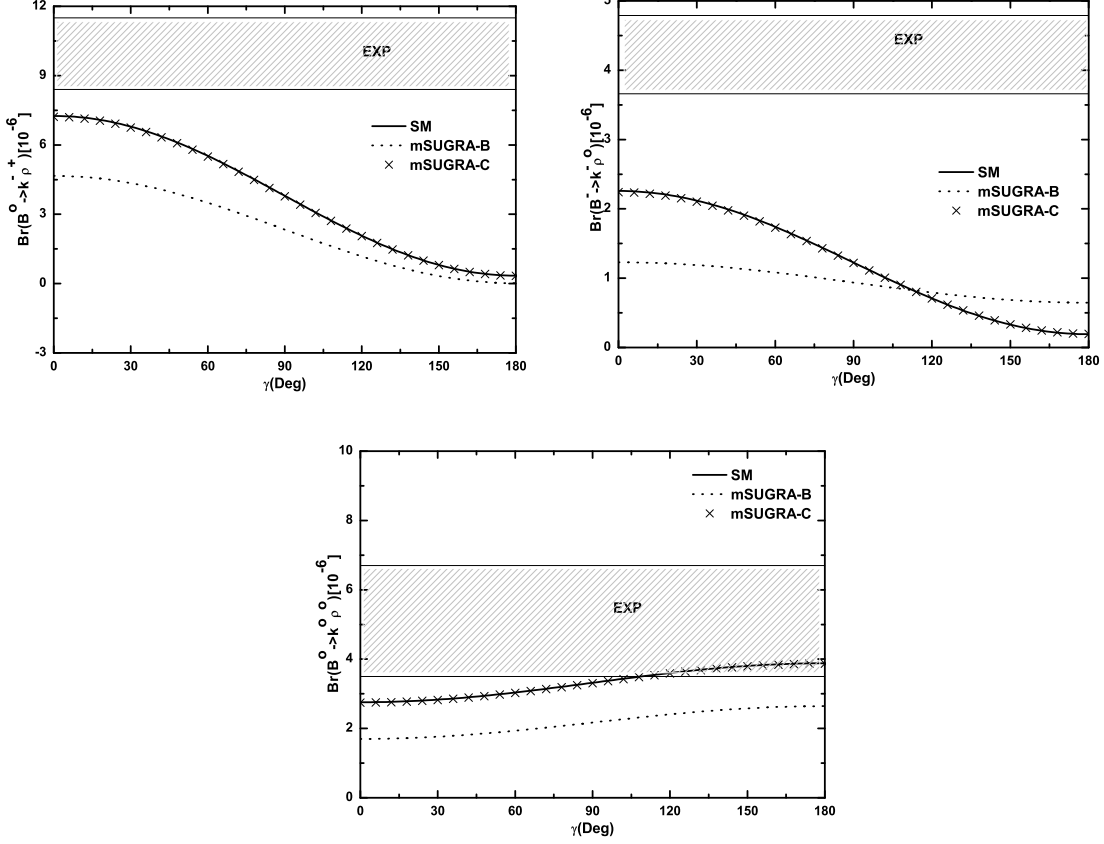


FIG. 4: The same as Fig.1 but for  $B \rightarrow K\rho$  decays.

$B \rightarrow K\rho$  decays respectively.

From Eqs.(28-30) and Fig. 4, one can see that the central values of the theoretical predictions in the SM and the mSUGRA model of case C are almost identical and about half of the measured values. In case B, unfortunately, the SUSY contribution produce a further forty percent variation in the “wrong” direction. But when we include the large errors induced by the uncertainties of  $\chi_A$ ,  $\overline{m}_s$  and form factors, the theoretical predictions in both the SM and the mSUGRA model (both Case B and Case C) can be consistent with the data.

For  $B \rightarrow K\omega$  decays, the situation is very similar to the  $B \rightarrow K\rho$  decays. From Eqs.(31-32) and Fig. 5, one can see that the central values of theoretical predictions in both the SM and the mSUGRA model are much smaller than the measured values. And the SUSY corrections in Case B even lead to a further reduction of the branching ratios.

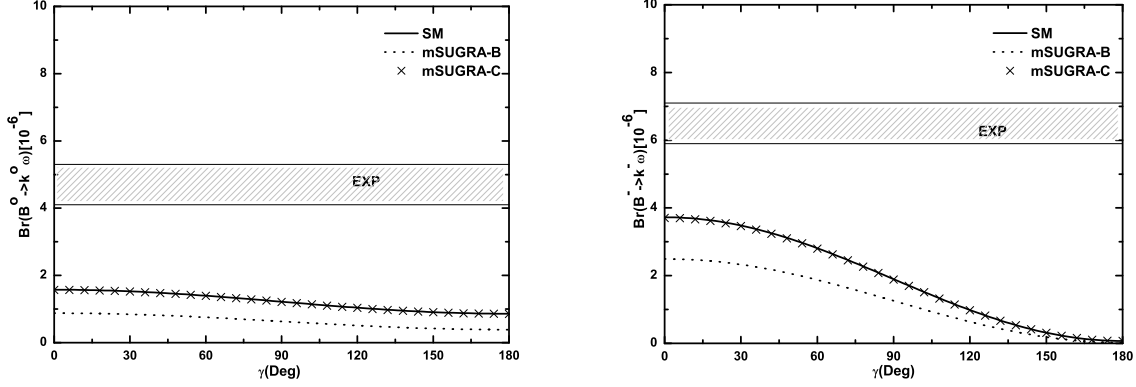


FIG. 5: The same as Fig.1 but for  $B \rightarrow K\omega$  decays.

The data and the theoretical predictions (in units of  $10^{-6}$ ) are

$$Br(\bar{B}^0 \rightarrow \bar{K}^0 \omega) = \begin{cases} 4.7 \pm 0.6, & \text{Data,} \\ 1.4 \pm 0.3(A_0^{B \rightarrow \omega})^{+1.3}_{-0.7}(\bar{m}_s)^{+3.0}_{-0.8}(\chi_A), & \text{SM,} \\ 0.8 \pm 0.1(A_0^{B \rightarrow \omega})^{+1.1}_{-0.5}(\bar{m}_s)^{+2.4}_{-0.6}(\chi_A), & \text{Case - B,} \\ 1.4 \pm 0.3(A_0^{B \rightarrow \omega})^{+1.3}_{-0.6}(\bar{m}_s)^{+3.0}_{-0.8}(\chi_A), & \text{Case - C,} \end{cases} \quad (31)$$

$$Br(B^- \rightarrow K^- \omega) = \begin{cases} 6.5 \pm 0.6, & \text{Data,} \\ 2.9 \pm 0.7(A_0^{B \rightarrow \omega})^{+0.5}_{-0.6}(\gamma)^{+1.8}_{-1.0}(\bar{m}_s)^{+3.7}_{-1.2}(\chi_A), & \text{SM,} \\ 1.9^{+0.5}_{-0.4}(A_0^{B \rightarrow \omega})^{+0.3}_{-0.4}(\gamma)^{+1.6}_{-0.8}(\bar{m}_s)^{+3.0}_{-0.9}(\chi_A), & \text{Case - B,} \\ 2.9 \pm 0.7(A_0^{B \rightarrow \omega})^{+0.4}_{-0.6}(\gamma)^{+1.8}_{-1.0}(\bar{m}_s)^{+3.7}_{-1.2}(\chi_A), & \text{Case - C.} \end{cases} \quad (32)$$

Here one can see that (a) the central values of the theoretical predictions in both the SM and mSUGRA model are all smaller than the data; and (b) the dominant error still comes from the uncertainty of the annihilation contributions and is very large in size.

#### 4. $B \rightarrow K^* \eta$ , $B \rightarrow \eta' \rho$

For the decay channels involving  $\eta^{(\prime)}$  meson, the dynamics is rather complex and has been studied by many authors, for example, in Refs. [12, 43]. Here we didn't consider the additional form-factor type contribution to the flavor-singlet coefficients  $\alpha_3^p(M_1 \eta_{q,s}^{(\prime)})$  (see Ref. [13]) since it has large uncertainties. The data and the theoretical predictions (in units of  $10^{-6}$ ) for the three measured decay modes in both the SM and the mSUGRA model are

$$Br(B^- \rightarrow K^{*-} \eta) = \begin{cases} 24.3^{+3.0}_{-2.9}, & \text{Data,} \\ 5.7^{+1.0}_{-0.9}(A_0^{B \rightarrow K^*})^{+1.0}_{-0.8}(\gamma)^{+3.7}_{-2.0}(\bar{m}_s)^{+9.0}_{-2.9}(\chi_A), & \text{SM,} \\ 6.4 \pm 0.8(A_0^{B \rightarrow K^*})^{+1.0}_{-0.8}(\gamma)^{+4.3}_{-2.3}(\bar{m}_s)^{+9.4}_{-3.1}(\chi_A), & \text{Case - B,} \\ 5.7^{+1.0}_{-0.9}(A_0^{B \rightarrow K^*})^{+1.0}_{-0.8}(\gamma)^{+3.7}_{-2.0}(\bar{m}_s)^{+9.0}_{-2.9}(\chi_A), & \text{Case - C,} \end{cases} \quad (33)$$

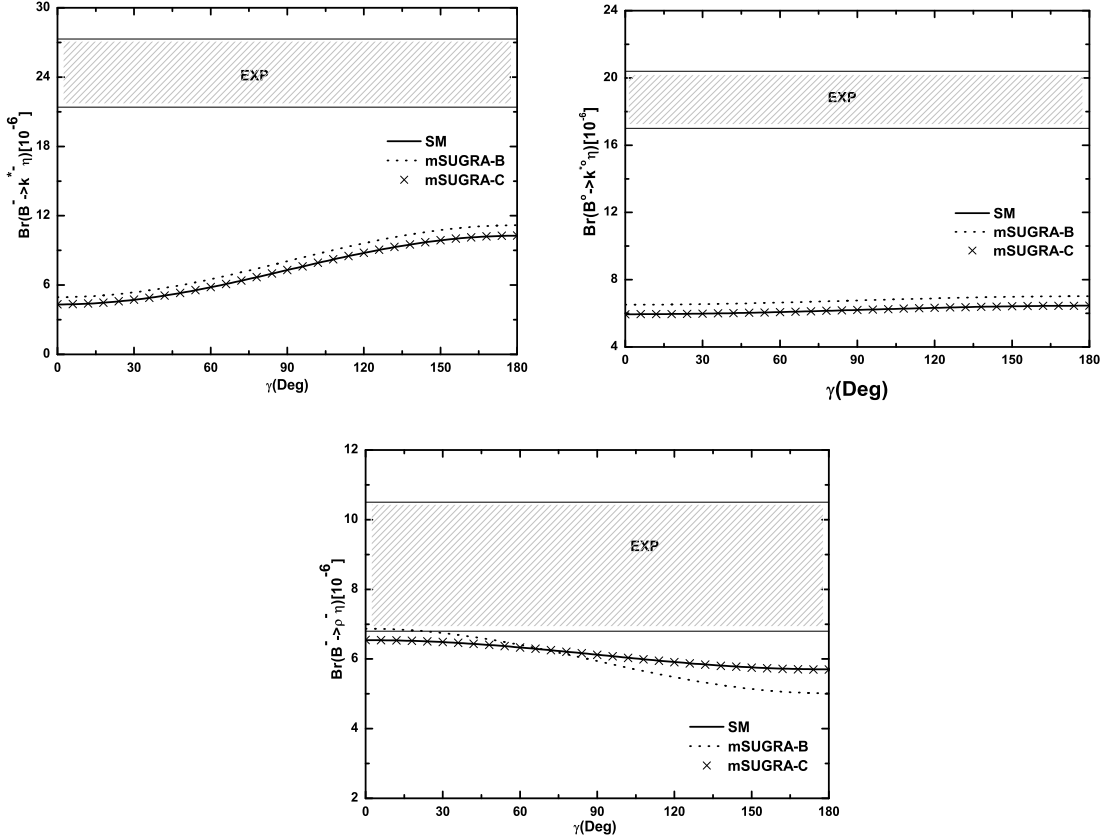


FIG. 6: The same as Fig.1 but for  $B \rightarrow K^* \eta$  and  $B^- \rightarrow \rho^- \eta$  decays.

$$Br(\bar{B}^0 \rightarrow \bar{K}^{*0} \eta) = \begin{cases} 18.7 \pm 1.7, & \text{Data,} \\ 6.1^{+1.0}_{-0.9}(A_0^{B \rightarrow K^*}) \pm 0.1(\gamma)^{+3.7}_{-2.0}(\bar{m}_s)^{+9.1}_{-3.0}(\chi_A), & \text{SM,} \\ 6.6 \pm 0.8(A_0^{B \rightarrow K^*}) \pm 0.1(\gamma)^{+4.2}_{-2.3}(\bar{m}_s)^{+9.5}_{-3.2}(\chi_A), & \text{Case - B,} \\ 6.1^{+1.0}_{-0.9}(A_0^{B \rightarrow K^*}) \pm 0.1(\gamma)^{+3.7}_{-2.0}(\bar{m}_s)^{+9.1}_{-3.0}(\chi_A), & \text{Case - C,} \end{cases} \quad (34)$$

$$Br(B^- \rightarrow \rho^- \eta) = \begin{cases} 8.6^{+1.9}_{-1.8}, & \text{Data,} \\ 6.3 \pm 0.2(\mu) \pm 0.1(\gamma) \pm 0.1(\bar{m}_s) \pm 0.3(\chi_A), & \text{SM,} \\ 6.4^{+0.2}_{-0.1}(\mu)^{+0.2}_{-0.3}(\gamma) \pm 0.1(\bar{m}_s) \pm 0.3(\chi_A), & \text{Case - B,} \\ 6.3 \pm 0.2(\mu) \pm 0.1(\gamma) \pm 0.1(\bar{m}_s) \pm 0.3(\chi_A), & \text{Case - C.} \end{cases} \quad (35)$$

Clearly the uncertainties of  $\chi_A$  and  $\bar{m}_s$  are the dominant error sources here.

By comparing the numerical results with the measured values, one finds that

- The SUSY contributions to these three measured decays are always small for both case B and C. For  $B^- \rightarrow K^* \eta$  and  $\bar{B}^0 \rightarrow \bar{K}^{*0} \eta$  decays, the central values of the theoretical predictions in both models are only around 30% of the measured values, and the data can be explained only when we take the large theoretical and

experimental errors into account. For  $B^- \rightarrow K^- \eta$  and  $\bar{B}^0 \rightarrow \bar{K}^0 \eta$  decays, however, the theoretical predictions in the SM and mSUGRA model as given in Ref. [26] agree well with the data.

- For  $B^- \rightarrow \rho^- \eta$  decay, a  $b \rightarrow d$  transition process, the SUSY contribution is very small, and the theoretical predictions in the SM and mSUGRA model are consistent with the data within one standard deviation.
- As illustrated in Fig. 6, the branching ratios of all the three channels have a weak dependence on the angle  $\gamma$ . For  $B \rightarrow K^* \eta$  decays, the theoretical errors are large in size and induced dominantly by the uncertainty of the parameter  $\chi_A$  and the mass  $\bar{m}_s$ . For  $B^- \rightarrow \rho^- \eta$  decay, however, the theoretical errors are relatively small.

## V. BRANCHING RATIOS FOR $B \rightarrow VV$ DECAYS

For  $B \rightarrow VV$  decay modes, one generally should evaluate three amplitudes with different helicity since they all can make contributions and do not interfere with each other. In terms of the helicity matrix elements

$$H_\lambda = \langle V_1(\lambda) V_2(\lambda) | H_{eff} | B \rangle, \quad \lambda = 0, \pm 1, \quad (36)$$

the branching ratios of  $B \rightarrow VV$  decays can be written as

$$Br(B \rightarrow V_1 V_2) = \tau_B \frac{|p_c|}{8\pi M_B^2} [|H_0|^2 + |H_{+1}|^2 + |H_{-1}|^2]. \quad (37)$$

The three independent helicity amplitudes  $H_0$ ,  $H_{+1}$  and  $H_{-1}$  can be expressed by three invariant amplitudes  $a_\lambda, b_\lambda, c_\lambda$  defined by the decomposition

$$H_\lambda = i\epsilon^\mu(\lambda)\eta^\nu(\lambda) \left[ a_\lambda g_{\mu\nu} + \frac{b_\lambda}{M_1 M_2} p_\mu p_\nu + \frac{ic_\lambda}{M_1 M_2} \epsilon_{\mu\nu\alpha\beta} p_1^\alpha p_2^\beta \right]. \quad (38)$$

Here  $\epsilon^\mu(\eta^\nu)$ ,  $p_{1,2}$  and  $M_{1,2}$  are the polarization vector, four momentum and masses of  $V_{1,2}$ , respectively, while  $p = p_1 + p_2$  is the four-momentum of B meson. The helicity elements  $H_\lambda$  can be further simplified as

$$\begin{aligned} H_{\pm 1} &= a_{\pm 1} \pm c_{\pm 1} \sqrt{x^2 - 1}, \quad H_0 = -a_0 x - b_0 (x^2 - 1) \\ x &= \frac{M_B^2 - M_1^2 - M_2^2}{2M_1 M_2} \end{aligned} \quad (39)$$

### A. Helicity amplitude of $B \rightarrow \rho^+ \rho^-$ , an example

Now we take the decay  $\bar{B}^0 \rightarrow \rho^\pm \rho^\mp$  as an example to show the ways of decomposition. With the QCD factorization approach, the decay amplitude of  $\bar{B}^0 \rightarrow \rho^\pm \rho^\mp$  decay reads

$$\begin{aligned} \mathcal{A}^\lambda(B \rightarrow \rho^+ \rho^-) &= -i \frac{G_F}{\sqrt{2}} f_\rho m_\rho \left[ (\varepsilon_+ \cdot \varepsilon_-) (m_B + m_\rho) A_1^{B \rightarrow \rho}(m_\rho^2) \right. \\ &\quad \left. - (\varepsilon_+ \cdot p_B)(\varepsilon_- \cdot p_B) \frac{2A_2^{B \rightarrow \rho}(m_\rho^2)}{m_B + m_\rho} - i \varepsilon_{\mu\nu\alpha\beta} \varepsilon_-^\mu \varepsilon_+^\nu p_B^\alpha p_+^\beta \frac{V^{B \rightarrow \rho}(m_\rho^2)}{m_B + m_\rho} \right] \\ &\quad \cdot [V_{ub} V_{ud}^* a_1^\lambda - V_{tb} V_{td}^* (a_4^\lambda + a_{10}^\lambda)] \end{aligned} \quad (40)$$

By comparing this expression of decay amplitude  $\mathcal{A}_\lambda$  with Eq.(38), one can find the coefficients  $a_\lambda, b_\lambda$  and  $c_\lambda$ ,

$$\begin{aligned} a_\lambda(B \rightarrow \rho^+ \rho^-) &= -\frac{G_F}{\sqrt{2}} f_\rho m_\rho (m_B + m_\rho) A_1^{B \rightarrow \rho}(m_\rho^2) \{V_{ub} V_{ud}^* a_1^\lambda - V_{tb} V_{td}^* [a_4^\lambda + a_{10}^\lambda]\}, \\ b_\lambda(B \rightarrow \rho^+ \rho^-) &= \sqrt{2} G_F f_\rho m_\rho^3 \frac{A_2^{B \rightarrow \rho}(m_\rho^2)}{m_B + m_\rho} \{V_{ub} V_{ud}^* a_1^\lambda - V_{tb} V_{td}^* [a_4^\lambda + a_{10}^\lambda]\}, \\ c_\lambda(B \rightarrow \rho^+ \rho^-) &= \sqrt{2} G_F f_\rho m_\rho^3 \frac{V^{B \rightarrow \rho}(m_\rho^2)}{m_B + m_\rho} \{V_{ub} V_{ud}^* a_1^\lambda - V_{tb} V_{td}^* [a_4^\lambda + a_{10}^\lambda]\}, \end{aligned} \quad (41)$$

where the factorized coefficients  $a_1^\lambda$ ,  $a_4^\lambda$  and  $a_{10}^\lambda$  can be written as

$$a_1^\lambda = C_1 + \frac{C_2}{N_c} + \frac{\alpha_s}{4\pi} \frac{C_F}{N_c} C_2 [f_I^\lambda + f_{II}^\lambda], \quad (42)$$

$$\begin{aligned} a_4^\lambda &= C_4 + \frac{C_3}{N_c} + \frac{\alpha_s}{4\pi} \frac{C_F}{N_c} C_3 [f_I^\lambda + f_{II}^\lambda] + \frac{\alpha_s}{4\pi} \frac{C_F}{N_c} \left\{ -C_1 \left[ \frac{v_u}{v_t} G^\lambda(s_u) + \frac{v_c}{v_t} G^\lambda(s_c) \right] \right. \\ &\quad + C_3 [G^\lambda(s_q) + G^\lambda(s_b)] + (C_4 + C_6) \sum_{q'=u}^b \left[ G^\lambda(s_{q'} - \frac{2}{3}) \right] + \frac{3}{2} C_9 [e_q G^\lambda(s_q) + \\ &\quad \left. e_b G^\lambda(s_b)] + \frac{3}{2} (C_8 + C_{10}) \sum_{q'=u}^b e_{q'} \left[ G^\lambda(s_{q'} - \frac{2}{3}) \right] + C_{8g} G_g^\lambda \right\}, \end{aligned} \quad (43)$$

$$a_{10}^\lambda = C_{10} + \frac{C_9}{N_c} + \frac{\alpha_s}{4\pi} \frac{C_F}{N_c} C_9 [f_I^\lambda + f_{II}^\lambda] - \frac{\alpha_e}{9\pi} C_e^\lambda, \quad (44)$$

In the above equations, the vertex corrections  $f_I^\lambda$  and the hard spectator scattering contributions  $f_{II}^\lambda$  are given by

$$f_I^0 = -12 \ln \frac{\mu}{m_b} - 18 + \int_0^1 du \Phi_{\parallel}^{V_2}(u) \left( 3 \frac{1-2u}{1-u} \ln u - 3i\pi \right), \quad (45)$$

$$f_I^\pm = -12 \ln \frac{\mu}{m_b} - 18 + \int_0^1 du \left( g_\perp^{(v)V_2}(u) \pm \frac{a g_\perp'^{(a)V_2}(u)}{4} \right) \left( 3 \frac{1-2u}{1-u} \ln u - 3i\pi \right), \quad (46)$$

$$f_{II}^0 = \frac{4\pi^2}{N_C} \frac{if_B f_{V_1} f_{V_2}}{h_0} \int_0^1 d\xi \frac{\Phi_1^B(\xi)}{\xi} \int_0^1 dv \frac{\Phi_{\parallel}^{V_1}(v)}{\bar{v}} \int_0^1 du \frac{\Phi_{\parallel}^{V_2}(u)}{u}, \quad (47)$$

$$\begin{aligned} f_{II}^\pm &= -\frac{4\pi^2}{N_C} \frac{2if_B f_{V_1}^\perp f_{V_2} m_{V_2}}{m_B h_\pm} (1 \mp 1) \int_0^1 d\xi \frac{\Phi_1^B(\xi)}{\xi} \int_0^1 dv \frac{\Phi_\perp^{V_1}(v)}{\bar{v}^2} \\ &\quad \times \int_0^1 du \left( g_\perp^{(v)V_2}(u) - \frac{g_\perp'^{(a)V_2}(u)}{4} \right) + \frac{4\pi^2}{N_C} \frac{2if_B f_{V_1} f_{V_2} m_{V_1} m_{V_2}}{m_B^2 h_\pm} \int_0^1 d\xi \frac{\Phi_1^B(\xi)}{\xi} \\ &\quad \times \int_0^1 dv du \left( g_\perp^{(v)V_1}(v) \pm \frac{g_\perp'^{(a)V_1}(v)}{4} \right) \left( g_\perp^{(v)V_2}(u) \pm \frac{g_\perp'^{(a)V_2}(u)}{4} \right) \frac{u + \bar{v}}{u\bar{v}^2}, \end{aligned} \quad (48)$$

here  $\bar{v} = 1 - v$  and the light-cone distribution amplitudes (LCDAS)  $\Phi_{\parallel}^V(u)$ ,  $\Phi_\perp^V(u)$ ,  $g_\perp^{(a)V}$ ,  $g_\perp^{(v)V}$  can be found in Ref. [41].

The functions describing the contributions of the QCD penguin-type diagrams, the dipole operator  $O_{8g}$  and the electro-weak penguin-type diagrams in eqs.(42-44) are [41]

$$G^0(s) = \frac{2}{3} - \frac{4}{3} \ln \frac{\mu}{m_b} + 4 \int_0^1 du \Phi_{\parallel}^{V_2}(u) g(u, s), \quad (49)$$

$$G^{\pm}(s) = \frac{2}{3} - \frac{2}{3} \ln \frac{\mu}{m_b} + 2 \int_0^1 du (g_{\perp}^{(v)V_2}(u) \pm \frac{g_{\perp}^{'(a)V_2}(u)}{4}) g(u, s), \quad (50)$$

$$G_g^0 = - \int_0^1 du \frac{2\Phi_{\parallel}^{V_2}(u)}{1-u}, \quad (51)$$

$$G_g^+ = - \int_0^1 du \left( g_{\perp}^{(v)V_2}(u) + \frac{g_{\perp}^{'(a)V_2}(u)}{4} \right) \frac{1}{1-u}, \quad (52)$$

$$G_g^- = \int_0^1 \frac{du}{\bar{u}} \left[ -\bar{u} g_{\perp}^{(v)V_2}(u) + \frac{\bar{u} g_{\perp}^{'(a)V_2}(u)}{4} + \int_0^u dv \left( \Phi_{\parallel}^{V_2}(v) - g_{\perp}^{(v)V_2}(v) \right) + \frac{g_{\perp}^{(a)V_2}(u)}{4} \right], \quad (53)$$

$$C_e^{\lambda} = \left[ \frac{v_u}{v_t} G^{\lambda}(s_u) + \frac{v_c}{v_t} G^{\lambda}(s_c) \right] \left( C_2 + \frac{C_1}{N_C} \right), \quad (54)$$

with the function  $g(u, s)$  defined as

$$g(u, s) = \int_0^1 dx x \bar{x} \ln(s - x \bar{x} \bar{u} - i\epsilon). \quad (55)$$

From Eq.(39), we can finally get the helicity elements  $H_{\pm 1}$  and  $H_0$ . One should note that the coefficients  $a, b$  and  $c$  are independent of the helicity  $\lambda$  in the naive factorization approach. In QCD factorization approach, however, the coefficients  $a_{\lambda}, b_{\lambda}$  and  $c_{\lambda}$  depend on the choice of  $\lambda$  ( $\lambda = 0, \pm 1$ ).

## B. Numerical results

Using the above formulae it is straightforward to calculate the branching ratios of  $B \rightarrow VV$  decays. In Table IV and V, we show the theoretical predictions for the CP-averaged branching ratios of the nineteen  $B \rightarrow VV$  decays in both the SM and the mSUGRA model, assuming  $\mu = m_b/2, m_b$  and  $2m_b$ , respectively.

In numerical calculations, we do not consider the annihilation contributions and only give  $Br^f$ . The reasons for this can be found in the last paragraph of Sec. III. Of course, the annihilation contribution may play an important role to explain the large transverse polarization of the  $B \rightarrow K^{*0} \rho^+$  and  $\phi K^{*+}$  decays, as pointed out in a recent paper [44], where the author has tried to include the contribution induced by a QCD penguin annihilation graph to explain the observed longitudinal polarization,  $f_L(B \rightarrow \phi K^*) \approx 50\%$ , in the framework of the SM. More studies are needed to understand this problem



TABLE IV: Numerical predictions in the SM and mSUGRA model (both case B and case C) for CP-averaged branching ratios in units of  $10^{-6}$  for  $b \rightarrow d$  transition processes of  $B \rightarrow VV$  decays, here the annihilation contributions are not included.

| $B \rightarrow VV$<br>( $b \rightarrow d$ ) | $\mu = m_b/2$ |        |       | $\mu = m_b$ |        |       | $\mu = 2m_b$ |        |       |
|---------------------------------------------|---------------|--------|-------|-------------|--------|-------|--------------|--------|-------|
|                                             | SM            | mSUGRA |       | SM          | mSUGRA |       | SM           | mSUGRA |       |
|                                             | $Br^f$        | (B)    | (C)   | $Br^f$      | (B)    | (C)   | $Br^f$       | (B)    | (C)   |
| $\bar{B}^0 \rightarrow \rho^+ \rho^-$       | 27.8          | 28.1   | 27.8  | 27.5        | 27.8   | 27.5  | 27.1         | 27.3   | 27.1  |
| $B^- \rightarrow \rho^- \rho^0$             | 18.4          | 18.4   | 18.4  | 18.7        | 18.7   | 18.7  | 19.1         | 19.1   | 19.1  |
| $B^- \rightarrow \rho^- \omega$             | 16.6          | 17.0   | 16.6  | 16.6        | 16.9   | 16.6  | 16.8         | 17.1   | 16.8  |
| $\bar{B}^0 \rightarrow \rho^0 \rho^0$       | 0.38          | 0.40   | 0.38  | 0.33        | 0.34   | 0.33  | 0.35         | 0.36   | 0.35  |
| $\bar{B}^0 \rightarrow \rho^0 \omega$       | 0.09          | 0.17   | 0.09  | 0.07        | 0.13   | 0.07  | 0.05         | 0.11   | 0.05  |
| $\bar{B}^0 \rightarrow \omega \omega$       | 0.40          | 0.44   | 0.40  | 0.33        | 0.37   | 0.33  | 0.33         | 0.37   | 0.34  |
| $\bar{B}^0 \rightarrow \rho^0 \phi$         | 0.004         | 0.004  | 0.004 | 0.003       | 0.003  | 0.003 | 0.003        | 0.003  | 0.003 |
| $B^- \rightarrow \rho^- \phi$               | 0.009         | 0.009  | 0.009 | 0.007       | 0.007  | 0.007 | 0.006        | 0.006  | 0.006 |
| $\bar{B}^0 \rightarrow \omega \phi$         | 0.003         | 0.003  | 0.003 | 0.003       | 0.003  | 0.003 | 0.002        | 0.002  | 0.002 |
| $\bar{B}^0 \rightarrow \bar{K}^{*0} K^{*0}$ | 0.28          | 0.46   | 0.28  | 0.22        | 0.37   | 0.22  | 0.17         | 0.30   | 0.18  |
| $B^- \rightarrow K^{*-} K^{*0}$             | 0.30          | 0.50   | 0.30  | 0.24        | 0.40   | 0.24  | 0.19         | 0.33   | 0.19  |

clearly. But it is beyond the scope of this paper, and we here just calculate the possible new physics contributions to the CP-averaged branching ratios of  $B \rightarrow VV$  decays in the mSUGRA model, and show the general pattern of such contributions.

From the numerical results as given in Table IV and V, one can see that the new physics contributions to the branching ratios of  $B \rightarrow VV$  decays are generally small for the SM-like case-C, but can be rather large for the case-B, especially to those penguin dominated  $B \rightarrow K^*(\rho, \omega, \phi)$  ( $b \rightarrow s$  transition) processes.

Among the nineteen  $B \rightarrow VV$  decays, only seven of them have been well measured, while upper limits are available for the remaining twelve decay modes. For the world average of the experimental measurements, one can see HFAG home page [42] and references therein. In the following subsections we focus on the seven measured decay channels.

TABLE V: Same as Table IV, but for  $b \rightarrow s$  transition processes of  $B \rightarrow VV$  decays.

| $B \rightarrow VV$<br>( $b \rightarrow s$ ) | $\mu = m_b/2$ |        |      | $\mu = m_b$ |        |      | $\mu = 2m_b$ |        |      |
|---------------------------------------------|---------------|--------|------|-------------|--------|------|--------------|--------|------|
|                                             | SM            | mSUGRA |      | SM          | mSUGRA |      | SM           | mSUGRA |      |
|                                             | $Br^f$        | (B)    | (C)  | $Br^f$      | (B)    | (C)  | $Br^f$       | (B)    | (C)  |
| $\bar{B}^0 \rightarrow K^{*-} \rho^+$       | 3.74          | 6.44   | 3.76 | 3.11        | 5.32   | 3.13 | 2.60         | 4.44   | 2.61 |
| $\bar{B}^0 \rightarrow \bar{K}^{*0} \rho^0$ | 0.81          | 1.90   | 0.82 | 0.57        | 1.42   | 0.57 | 0.38         | 1.04   | 0.38 |
| $B^- \rightarrow K^{*-} \rho^0$             | 4.43          | 6.63   | 4.44 | 3.87        | 5.74   | 3.88 | 3.40         | 5.02   | 3.41 |
| $B^- \rightarrow K^{*0} \rho^-$             | 5.38          | 9.15   | 5.41 | 4.36        | 7.51   | 4.38 | 3.48         | 6.14   | 3.50 |
| $\bar{B}^0 \rightarrow K^{*0} \omega$       | 2.35          | 3.76   | 2.36 | 1.90        | 3.12   | 1.90 | 1.50         | 2.58   | 1.51 |
| $B^- \rightarrow K^{*-} \omega$             | 2.02          | 3.19   | 2.03 | 1.70        | 2.71   | 1.71 | 1.45         | 2.32   | 1.45 |
| $\bar{B}^0 \rightarrow K^{*0} \phi$         | 5.61          | 9.91   | 5.64 | 4.24        | 7.82   | 4.26 | 3.13         | 6.15   | 3.15 |
| $B^- \rightarrow K^{*-} \phi$               | 6.09          | 10.76  | 6.12 | 4.60        | 8.50   | 4.63 | 3.40         | 6.68   | 3.42 |

1.  $\bar{B}^0 \rightarrow \rho^+ \rho^-$ ,  $B^- \rightarrow \rho^- (\rho^0, \omega)$

These three decays are tree-dominated decay channels. The data and the theoretical predictions of the branching ratios (in units of  $10^{-6}$ ) in the SM and mSUGRA model are

$$Br(\bar{B}^0 \rightarrow \rho^+ \rho^-) = \begin{cases} 26.2^{+3.6}_{-3.7}, & \text{Data,} \\ 27.5^{+4.1}_{-3.8}(A^{B \rightarrow \rho})^{+1.1}_{-1.4}(\gamma), & \text{SM,} \\ 27.8^{+4.1}_{-3.8}(A^{B \rightarrow \rho})^{+1.4}_{-1.8}(\gamma), & \text{Case - B,} \\ 27.5^{+4.1}_{-3.8}(A^{B \rightarrow \rho})^{+1.1}_{-1.4}(\gamma), & \text{Case - C,} \end{cases} \quad (56)$$

$$Br(B^- \rightarrow \rho^- \rho^0) = \begin{cases} 26.4^{+6.1}_{-6.4}, & \text{Data,} \\ 18.7^{+2.5}_{-2.3}(A^{B \rightarrow \rho})^{+0.3}_{-0.4}(\gamma), & \text{SM,} \\ 18.7^{+2.5}_{-2.3}(A^{B \rightarrow \rho})^{+0.3}_{-0.4}(\gamma), & \text{Case - B,} \\ 18.7^{+2.5}_{-2.3}(A^{B \rightarrow \rho})^{+0.3}_{-0.4}(\gamma), & \text{Case - C,} \end{cases} \quad (57)$$

$$Br(B^- \rightarrow \rho^- \omega) = \begin{cases} 12.6^{+4.0}_{-3.7}, & \text{Data,} \\ 16.6^{+2.3}_{-2.1}(A^{B \rightarrow \omega})^{+1.0}_{-1.4}(\gamma), & \text{SM,} \\ 16.9^{+2.3}_{-2.2}(A^{B \rightarrow \omega})^{+1.4}_{-1.8}(\gamma), & \text{Case - B,} \\ 16.6^{+2.3}_{-2.1}(A^{B \rightarrow \omega})^{+1.1}_{-1.4}(\gamma), & \text{Case - C.} \end{cases} \quad (58)$$

Here the dominant errors also come from the uncertainties of the form factors and the angle  $\gamma$ .

Fig. 7 shows the  $\gamma$  dependence of the branching ratios for the three decays in the SM and the mSUGRA model. From this figure and the numerical results as given in Eqs.(56-58), we can easily find that the SUSY contributions to these tree-dominated decays are very small. The largest error here still comes from the uncertainty of the relevant form factors, and the theoretical predictions in both the SM and mSUGRA model are consistent with the data within one standard deviation.

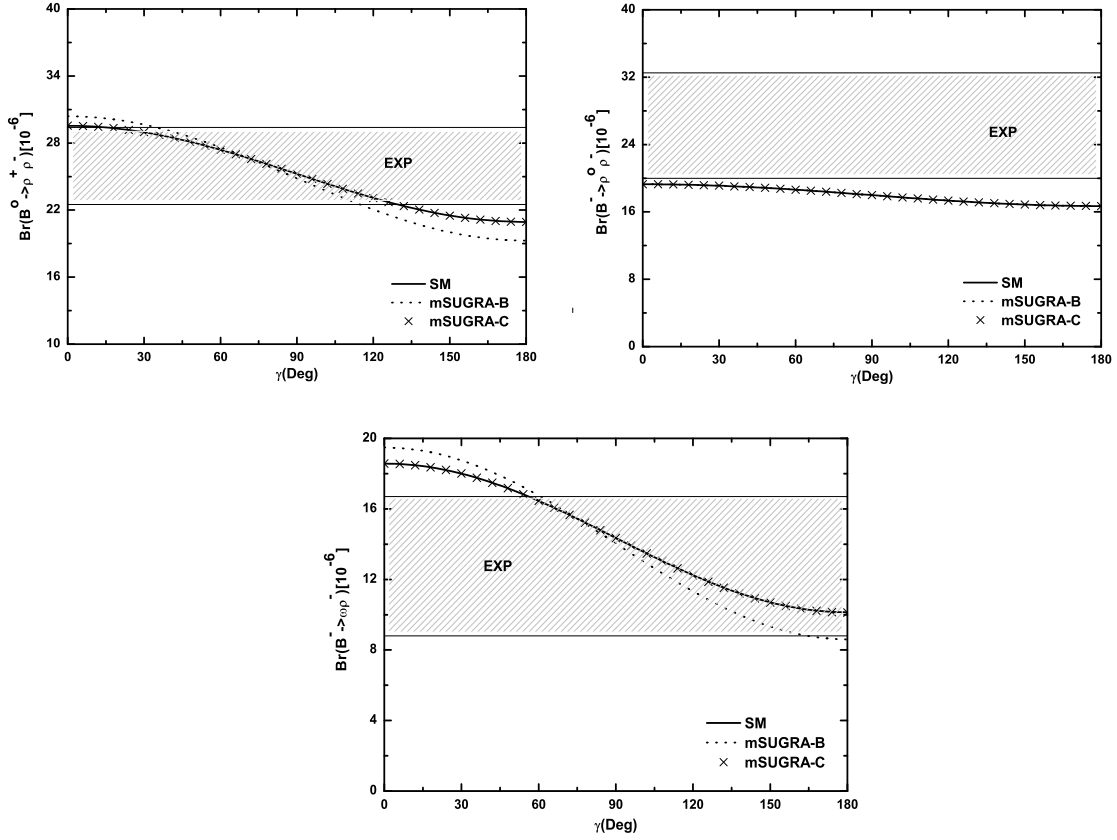


FIG. 7: The same as Fig.1 but for  $B^0 \rightarrow \rho^+ \rho^-$  and  $B^- \rightarrow \rho^- (\rho^0, \omega)$  decays.

2.  $B^- \rightarrow K^{*-} \rho^0$ ,  $K^{*0} \rho^-$  and  $B \rightarrow K^* \phi$

Since these four decays are penguin dominated decay modes, the SUSY contributions may be significant. The world averages, the theoretical predictions (all in units of  $10^{-6}$ ) in the SM and the mSUGRA model are

$$Br(B^- \rightarrow K^{*-} \rho^0) = \begin{cases} 10.6^{+3.8}_{-3.5}, & \text{Data,} \\ 3.9^{+0.6}_{-0.5}(\mu) \pm 0.4(A^{B \rightarrow \rho})^{+0.5}_{-0.4}(A^{B \rightarrow K^*})^{+1.5}_{-1.2}(\gamma), & \text{SM,} \\ 5.7^{+0.9}_{-0.7}(\mu) \pm 0.6(A^{B \rightarrow \rho}) \pm 0.6(A^{B \rightarrow K^*})^{+1.8}_{-1.4}(\gamma), & \text{Case - B,} \\ 3.9^{+0.6}_{-0.5}(\mu) \pm 0.4(A^{B \rightarrow \rho})^{+0.5}_{-0.4}(A^{B \rightarrow K^*})^{+1.5}_{-1.2}(\gamma), & \text{Case - C,} \end{cases} \quad (59)$$

$$Br(B^- \rightarrow K^{*0} \rho^-) = \begin{cases} 10.6 \pm 1.9, & \text{Data,} \\ 4.4^{+1.0}_{-0.9}(\mu)^{+0.7}_{-0.6}(A^{B \rightarrow \rho})^{+0.01}_{-0.02}(\gamma), & \text{SM,} \\ 7.5^{+1.6}_{-1.4}(\mu) \pm 1.1(A^{B \rightarrow \rho}) \pm 0.02(\gamma), & \text{Case - B,} \\ 4.4^{+1.0}_{-0.9}(\mu)^{+0.7}_{-0.6}(A^{B \rightarrow \rho})^{+0.01}_{-0.02}(\gamma), & \text{Case - C,} \end{cases} \quad (60)$$

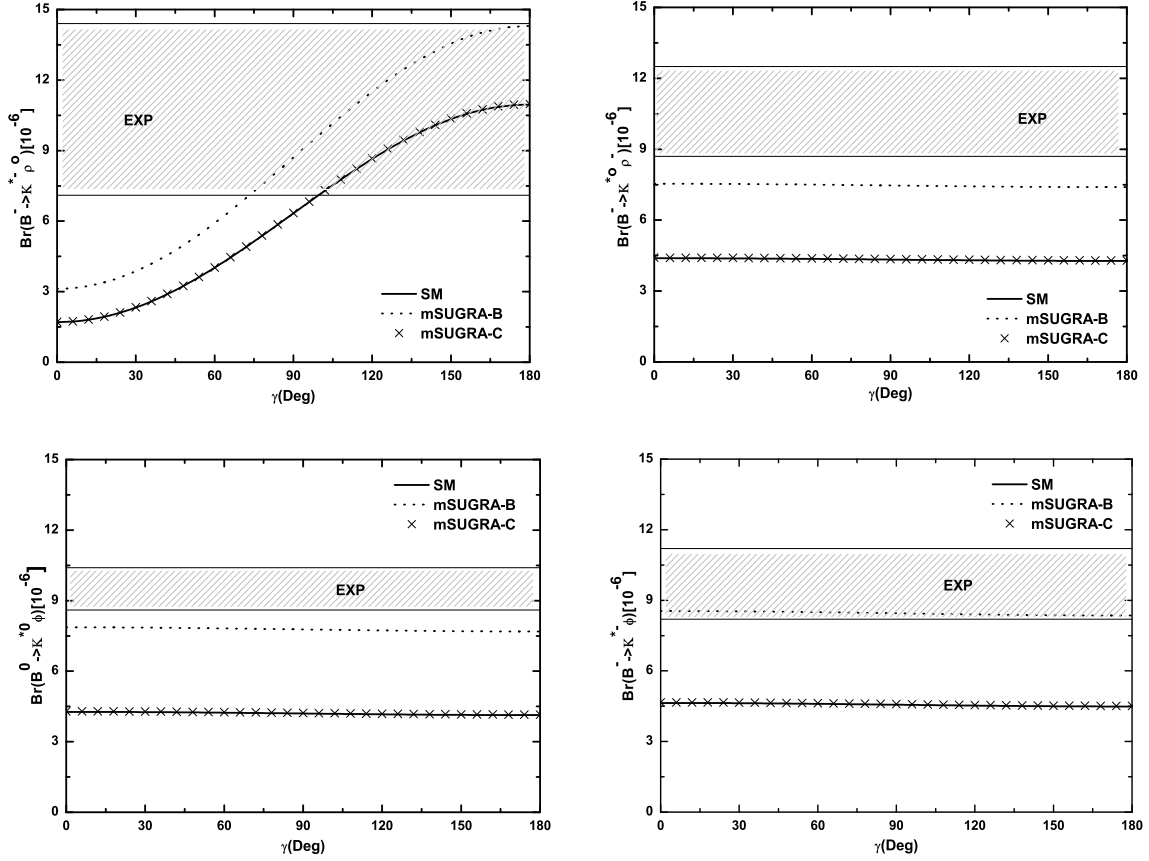


FIG. 8: The same as Fig.1 but for  $B^- \rightarrow K^{*-} \rho^0$ ,  $K^{*0} \rho^-$  and  $B \rightarrow K^* \phi$  decays.

$$Br(\bar{B}^0 \rightarrow \bar{K}^{*0} \phi) = \begin{cases} 9.5 \pm 0.9, & \text{Data,} \\ 4.2^{+1.4}_{-1.1}(\mu) + 1.7^{+1.7}_{-1.5}(A^{B \rightarrow K^*}) \pm 0.02(\gamma), & \text{SM,} \\ 7.8^{+2.1}_{-1.7}(\mu) + 3.1^{+3.1}_{-2.6}(A^{B \rightarrow K^*}) + 0.02^{+0.02}_{-0.03}(\gamma), & \text{Case - B,} \\ 4.3^{+1.4}_{-1.1}(\mu) + 1.8^{+1.8}_{-1.5}(A^{B \rightarrow K^*}) \pm 0.02(\gamma), & \text{Case - C,} \end{cases} \quad (61)$$

$$Br(B^- \rightarrow K^{*-} \phi) = \begin{cases} 9.7 \pm 1.5, & \text{Data,} \\ 4.6^{+1.5}_{-1.2}(\mu) + 1.9^{+1.9}_{-1.6}(A^{B \rightarrow K^*}) \pm 0.02(\gamma), & \text{SM,} \\ 8.5^{+2.3}_{-1.8}(\mu) + 3.4^{+3.4}_{-2.8}(A^{B \rightarrow K^*}) + 0.02^{+0.02}_{-0.03}(\gamma), & \text{Case - B,} \\ 4.6^{+1.5}_{-1.2}(\mu) + 1.9^{+1.9}_{-1.6}(A^{B \rightarrow K^*}) \pm 0.02(\gamma), & \text{Case - C.} \end{cases} \quad (62)$$

Here the major errors are induced by the uncertainties of the input parameters  $\mu$ ,  $A^{B \rightarrow \rho}$ ,  $A^{B \rightarrow K^*}$  and the angle  $\gamma$ .

From the numerical results as given in Eqs.(59-62) and Fig. 8, one can see that

- For these four channels, the central values of the SM predictions are less than half of the measured values. The SUSY contributions are negligibly small for the case C, but can provide a 70% enhancements for case C.

- The dominant errors still come from the uncertainty of the form factors and the renormalization scale  $\mu$ . Except for the decay  $B^- \rightarrow K^{*-}\rho^0$ , other three decays are almost independent of the angle  $\gamma$ . The reason is that the latter three decays are pure penguin processes and have no terms proportional to  $V_{td}$  or  $V_{ub}$ .

## VI. SUMMARY

In this paper, we calculated the new physics contributions to the CP-averaged branching ratios of the thirty nine  $B \rightarrow PV$  and nineteen  $B \rightarrow VV$  decay channels in the mSUGRA model by employing the QCD factorization approach.

In Sec. II, a brief review about the mSUGRA model and the SUSY corrections to the Wilson coefficients was given. In Sec. III, we presented a short discussion about the QCD factorization approach which is commonly used to evaluate the hadronic matrix elements  $\langle M_1 M_2 | O_i | B \rangle$ . In Sec. IV and Sec. V, we calculated the branching ratios of  $B \rightarrow PV$  and  $B \rightarrow VV$  decays in the SM and the mSUGRA model, and made phenomenological analysis for those well-measured decay modes.

In the mSUGRA model, the Wilson coefficient  $C_{7\gamma}(m_b)$  can be either SM-like or sign-flipped comparing with that in the SM. The data of  $B \rightarrow X_s \gamma$  can provide a strong constraint on the size of  $C_{7\gamma}(m_b)$ , but not its sign. The latest measurements of  $B \rightarrow X_s l^+ l^-$  decay prefer a negative (SM-like)  $C_{7\gamma}(m_b)$ . In this paper we choose three typical sets of the mSUGRA input parameters ( $m_0, m_{\frac{1}{2}}, A_0, \tan \beta, \text{Sign}(\mu)$ ) in which  $C_{7\gamma}(m_b)$  can be either SM-like (the case A and C) or have a flipped-sign (the case B).

As expected, the SUSY contributions to all channels considered here are very small for both the SM-like case A and C. For case B, however, the SUSY contributions can be significant for those penguin-dominated decays, and for this case we found that

- For those tree-dominated decays or the decay channels having the penguin contribution only coming from  $\alpha_3, \alpha_3^{ew}$  or having only weak annihilation contribution, the SUSY contributions in case B are also very small.
- For those QCD penguin-dominated decay modes, the SUSY contributions can interfere with the corresponding SM parts constructively or destructively, and consequently can provide an enhancement about 30%  $\sim$  260% to the branching ratios of the decays  $B \rightarrow \pi K^*, K\phi, K^*\phi, K^*\rho$  etc, or a reduction about 30%  $\sim$  80% to the branching ratios of the decays  $B \rightarrow K\rho, K\omega$  etc.
- For  $B \rightarrow K^*(\pi, \rho)$  and  $B \rightarrow (K, K^*)\phi$  decays, the central values of the SM predictions for branching ratios are generally less than half of the measured values. But the mSUGRA predictions can become consistent with the data within one standard deviation due to the inclusion of the significant SUSY enhancements.
- For  $B \rightarrow K\rho$  and  $B \rightarrow K\omega$  decays, the SUSY contributions interfere with their SM parts destructively, more investigations are needed to cover the gap between the theoretical predictions and the data.
- For most decay channels, the error induced by the uncertainty of the annihilation contributions is dominant and large in size. The SM predictions, consequently, have

large theoretical errors when the QCD factorization approach is employed. The large SUSY contributions in the case B, unfortunately, may be masked by the large theoretical errors dominated by the uncertainty from our ignorance of calculating the annihilation contributions in the QCD factorization approach. Hence we expect the theory will go further to make the annihilation contributions calculated reliably and only at that time can one distinguish the new physics contributions from the theoretical errors.

In short, only in case B, can the SUSY contributions be significant to the branching ratios of the studied B meson decays. If the sign of  $C_{7\gamma}(m_b)$  can be strictly determined to be SM-like finally, as claimed firstly in Ref. [37], the parameter space of the mSUGRA model will be strongly restricted, and the branching ratios of the two-body charmless B decays can hardly be affected.

### Acknowledgments

We are very grateful to Cai-dian Lü and Li-bo Guo for helpful discussions. This work is partially supported by the National Natural Science Foundation of China under Grant No.10275035 and 10575052, and by the Research Foundation of Nanjing Normal University under Grant No. 214080A916.

### APPENDIX A: INPUT PARAMETERS

In this appendix we present the relevant input parameters being used in our numerical calculations.

- Decay constants. The decay constants are defined by following current matrix elements[45]:

$$\langle P(q) | \bar{q} \gamma_\mu \gamma_5 q | 0 \rangle = -i f_P q_\mu, \quad \langle V(q, \epsilon) | \bar{q} \gamma_\mu q | 0 \rangle = f_V m_V \epsilon^{*\mu}. \quad (\text{A1})$$

And the scale-dependent transverse decay constant in Eq.(13) is defined as[13]

$$\langle V(q, \epsilon^*) | \bar{q} \sigma_{\mu\nu} q | 0 \rangle = f_V^\perp (q_\mu \epsilon_\nu^* - q_\nu \epsilon_\mu^*), \quad (\text{A2})$$

where  $\epsilon_\mu^*$  denotes the polarization vector of the vector meson V. These decay constants are nonperturbative parameters. And they can be extracted from the experimental data or estimated with well-founded theories, such as QCD sum rules, etc. The decay constants we used here, in units of  $MeV$ , are

| $f_\pi$ | $f_K$ | $f_B$ | $f_\rho$ | $f_{K^*}$ | $f_\omega$ | $f_\phi$ | $f_\rho^\perp$ | $f_{K^*}^\perp$ | $f_\omega^\perp$ | $f_\phi^\perp$ |
|---------|-------|-------|----------|-----------|------------|----------|----------------|-----------------|------------------|----------------|
| 131     | 160   | 200   | 209      | 218       | 187        | 221      | 150            | 175             | 150              | 175            |

As to the decay constants related to  $\eta$  and  $\eta'$ , we shall take the convention in Ref. [8]:

$$\langle 0 | \bar{q} \gamma_\mu \gamma_5 q | \eta^{(\prime)}(p) \rangle = -i f_{\eta^{(\prime)}}^q p_\mu \quad (\text{A3})$$

the quantities  $f_{\eta^{(\prime)}}^u$  and  $f_{\eta^{(\prime)}}^s$  in the two-angle mixing formalism are

$$f_{\eta'}^u = \frac{f_8}{\sqrt{6}} \sin \theta_8 + \frac{f_0}{\sqrt{3}} \cos \theta_0, \quad f_{\eta'}^s = -2 \frac{f_8}{\sqrt{6}} \sin \theta_8 + \frac{f_0}{\sqrt{3}} \cos \theta_0 \quad (\text{A4})$$

$$f_{\eta}^u = \frac{f_8}{\sqrt{6}} \cos \theta_8 - \frac{f_0}{\sqrt{3}} \sin \theta_0, \quad f_{\eta}^s = -2 \frac{f_8}{\sqrt{6}} \cos \theta_8 - \frac{f_0}{\sqrt{3}} \sin \theta_0 \quad (\text{A5})$$

with  $f_8 = 1.28f_\pi$ ,  $f_0 = 1.2f_\pi$ ,  $\theta_0 = -9.1^\circ$  and  $\theta_8 = -22.2^\circ$ . In order to incorporate the charm-loop diagram contribution into  $\eta^{(\prime)}$  involved decays, two new decay constants should be given, namely  $f_\eta^c$  and  $f_{\eta'}^c$ . Following Ref. [12], we take values  $f_\eta^c \simeq -1\text{MeV}$  and  $f_{\eta'}^c \simeq -3\text{MeV}$ .

- Form factors. The form factors are in nature nonperturbative quantities, extracted usually from the experimental measurements. In Ref. [45], the form factors were defined by current matrix elements

$$\begin{aligned} \langle P(q) | \bar{q} \gamma^\mu (1 - \gamma_5) q | B \rangle &= \left[ p_B^\mu + q^\mu - \frac{m_B^2 - m_P^2}{k^2} k^\mu \right] F_1(k^2) \\ &+ \frac{m_B^2 - m_P^2}{k^2} k^\mu F_0(k^2), \end{aligned} \quad (\text{A6})$$

$$\begin{aligned} \langle V(q, \epsilon) | \bar{q} \gamma_\mu (1 - \gamma_5) q | B \rangle &= \epsilon_{\mu\nu\alpha\beta} \epsilon^{*\nu} p_B^\alpha q^\beta \frac{2V(k^2)}{m_B + m_V} + i \frac{2m_V(\epsilon^* \cdot k)}{k^2} k_\mu A_0(k^2) \\ &+ i \epsilon_\mu^* (m_b + m_V) A_1(k^2) - i \frac{\epsilon^* \cdot k}{m_b + m_V} (p_B + q)_\mu A_2(k^2) \\ &- i \frac{2m_V(\epsilon^* \cdot k)}{k^2} k_\mu A_3(k^2), \end{aligned} \quad (\text{A7})$$

where  $k = p_B - q$ . We neglect corrections to the decay amplitudes quadratic in the light meson masses, so that all form factors are evaluated at  $k^2 = 0$ . At the poles  $k^2 = 0$ , we have

$$F_0(0) = F_1(0), \quad A_0(0) = A_3(0), \quad (\text{A8})$$

$$2m_V A_3(0) = (m_B + m_V) A_1(0) - (m_B - m_V) A_2(0). \quad (\text{A9})$$

In our calculations, we use the form factors as given in Refs. [13, 46]. They are

|       | $B \rightarrow \pi$ | $B \rightarrow K$ | $B \rightarrow \rho$ | $B \rightarrow K^*$ | $B \rightarrow \omega$ |
|-------|---------------------|-------------------|----------------------|---------------------|------------------------|
| $F_0$ | $0.28 \pm 0.05$     | $0.34 \pm 0.05$   | —                    | —                   | —                      |
| $A_0$ | —                   | —                 | $0.37 \pm 0.06$      | $0.45 \pm 0.07$     | $0.33 \pm 0.05$        |
| $A_1$ | —                   | —                 | $0.242 \pm 0.02$     | $0.292 \pm 0.06$    | $0.219 \pm 0.02$       |
| $A_2$ | —                   | —                 | $0.221 \pm 0.02$     | $0.259 \pm 0.06$    | $0.198 \pm 0.02$       |
| $V$   | —                   | —                 | $0.323 \pm 0.03$     | $0.411 \pm 0.08$    | $0.293 \pm 0.03$       |

For the form factors of  $B \rightarrow \eta$  and  $B \rightarrow \eta'$  transitions, we use [8]

$$F_{0,1}^{B \rightarrow \eta} = F_{0,1}^{B \rightarrow \pi} \left( \frac{\cos \theta_8}{\sqrt{6}} - \frac{\sin \theta_0}{\sqrt{3}} \right), \quad F_{0,1}^{B \rightarrow \eta'} = F_{0,1}^{B \rightarrow \pi} \left( \frac{\sin \theta_8}{\sqrt{6}} + \frac{\cos \theta_0}{\sqrt{3}} \right). \quad (\text{A10})$$

- The parameters  $\chi_{H,A}$ . When calculating the contribution from hard spectator scattering and annihilation diagrams, the end point divergence will appear. To treat the divergence, one can parameterize them by  $\chi_H$  and  $\chi_A$  respectively [11].

In numerical calculations, we set  $\rho_H = \rho_A = 0$  as the default input values [11]. And we also scan over  $\rho_A \in [0, 1]$  and  $\phi_A \in [-180^\circ, 180^\circ]$  to estimate the theoretical error induced by the uncertainty of the annihilation contributions.

- In this paper, we use the same CKM angles, quark masses, meson masses and the B meson lifetimes as used in Ref. [26].



- 
- [1] Belle Collab., Y. Chao, et al, Phys. Rev. Lett. **93**, 191802 (2004); Phys. Rev. D **71**, 031502 (2005); Belle Collab., J.Zhang, et al, Phys. Rev. Lett. **94**, 031801 (2005).
  - [2] BaBar Collab., B. Aubert, et al, Phys. Rev. Lett. **93**, 131801 (2004);
  - [3] A.I. Sanda, talk given at LHC 2004, July 2004, Vienna, Austria.
  - [4] *The Babar Physics Book*, edited by P.F. Harrison and H.R. Quinn, Report No. SLAC-R-504, 1998.
  - [5] T. Hurth, Rev. Mod. Phys. **75**, 1159(2003); A.J. Buras, R. Fleischer, S. Recksiegel and F. Schwab, Phys. Rev. Lett. **92**, 101804 (2004); Eur. Phys. J. C **32**, 45 (2003); and Nucl. Phys. B **697**, 133 (2004).
  - [6] M. Gronau and J.L. Rosner, Phys. Lett. B **572**, 43 (2003).
  - [7] M. Ciuchini and L. Silvestrini, Phys. Rev. Lett. **89**, 231802 (2002); C.W. Chiang and J.L. Rosner, Phys. Rev. D **68**, 014007 (2003); C.S. Huang and S.H. Zhu, Phys. Rev. D **68**, 114020 (2003); J.F. Cheng, C.S. Huang, and X.H. Wu, Phys. Lett. B **585**, 287 (2004); S. Mishima, A.I. Sanda, Phys. Rev. D **69**, 054005 (2004); O. Tajima, talk given at the 2005 Aspen Winter Conference, Feb.18, 2005, Aspen, US.
  - [8] A. Ali, G. Kramer and C.D. Lü, Phys. Rev. D **58**, 094009 (1998).
  - [9] Y.H. Chen, H.Y. Cheng, B. Tseng and K.C. Yang, Phys. Rev. D **60**, 094014 (1999).
  - [10] D.S. Du, H.J. Gong, J.F. Sun, D.S. Yang and G.H. Zhu, Phys. Rev. D **65**, 074001(2002); *ibid* Phys. Rev. D **65**, 094025 (2002); Phys. Rev. D **66**, 079904 (E) (2002).
  - [11] M. Beneke, G. Buchalla, M. Neubert and C.T. Sachrajda, Nucl. Phys. B **606**, 245 (2001).
  - [12] M. Beneke and M. Neubert, Nucl. Phys. B **651**, 225 (2003).
  - [13] M. Beneke and M. Neubert, Nucl. Phys. B **675**, 333 (2003).
  - [14] Y.Y. Keum, H.n. Li and A.I. Sanda, Phys. Rev. D **63**, 054008 (2001); Y.Y. Keum and H.n. Li, Phys. Rev. D **63**, 074006 (2001); C.D. Lü, K. Ukai and M.Z. Yang, Phys. Rev. D **63**, 074009(2001); C.D. Lü and M.Z. Yang, Eur. Phys. J. C **23**, 275(2002); Y. Li, C.D. Lü, Z.J. Xiao and X.Q. Yu, Phys. Rev. D **70**, 034009 (2004); Y. Li, C.D. Lü and Z.J. Xiao, J. Phys. G **31**, 273 (2005); X. Liu, W.S. Wang, Z.J. Xiao, L.B. Guo, and C.D.Lü, hep-ph/0509362.
  - [15] Z.J. Xiao, W.J. Li, L.B. Guo and G.R. Lu, Eur. Phys. J. C **18**, 681 (2001); Z.J. Xiao, C.D. Lü and W.J. Huo, Phys. Rev. D **67**, 094021 (2003).
  - [16] Z.J. Xiao, C.S. Li and K.T. Chao, Phys. Rev. D **63**, 074005 (2001); Z.J. Xiao, K.T. Chao and C.S. Li, Phys. Rev. D **65**, 114021 (2002) and references therein.
  - [17] D. Atwood, L. Reina, and A. Soni, Phys. Rev. D **55**, 3156 (1997); F.M. Borzumati and C. Greub, Phys. Rev. D **58**, 074004 (1998); T.M. Aliev and E.O. Iltan, J. Phys. G **25**, 989 (1999); D. Bowser-Chao, K. Cheung, and W.Y. Keung, Phys. Rev. D **59**, 115006 (1999); Y.B. Dai, C.S. Huang and H.W. Huang, Phys. Lett. B **390**, 257 (1997); C.S. Huang, W. Liao, Q.S. Yan and S.H. Zhu, Phys. Rev. D **63**, 114021 (2001); J.J. Cao, Z.J. Xiao and G.R. Lu, Phys. Rev. D **64**, 014012 (2001); D. Zhang, Z.J. Xiao and C.S. Li, Phys. Rev. D **64**, 014014 (2001).
  - [18] H. Baer, M. Brhlik, D. Castaño and X. Tata, Phys. Rev. D **58**, 015007 (1998); H. Baer and M. Brhlik, Phys. Rev. D **55**, 3201 (1997).
  - [19] T. Goto, T. Nihei and Y. Okada, Phys. Rev. D **53**, 5233 (1996); *ibid* **54**, 5904 (E) (1996).
  - [20] T. Goto, Y. Okada, Y. Shimizu and M. Tanaka, Phys. Rev. D **55**, 4273 (1997); *ibid* **66**,

- 019901 (E) (2002).
- [21] H.H. Asatryan, H.M. Asatryan, Phys. Lett. B **460**, 148 (1999); A. Ali, P. Ball, L.T. Handoko, G. Hiller, Phys. Rev. D **61**, 074024 (2000); C. Bobeth, A.J. Buras, F. Kruger, J. Urban, Nucl. Phys. B **630**, 87 (2002); J.F. Cheng, C.S. Huang and X.H. Wu, Nucl. Phys. B **701** (2004) 54.
  - [22] S. Khalil and E. Kou, Phys. Rev. D **71**, 114016 (2005); E. Gabrielli, K. Huitu, and S. Khalil, Nucl. Phys. B **710**, 139 (2005); S. Khalil, Phys. Rev. D **72**, 035007(2005).
  - [23] R. Barbieri, S. Ferrara and C.A. Savoy, Phys. Lett. B **119**, 343(1982); A.H.Chamseddine, R. Arnowitt and P. Nath, Phys. Rev. Lett. **49**, 970 (1982); L. Hall, J. Lykken and S. Weinberg, Phys. Rev. D **27**, 2359 (1983); N. Ohta, Prog. Theor. Phys. **70** (1983) 542.
  - [24] A. Djouadi *et al.*, *The minimal supersymmetric standard model: Group summery report*, hep-ph/9901246.
  - [25] C.S. Huang and X.H. Wu, Nucl. Phys. B **657**, 304 (2003).
  - [26] Z.J. Xiao and W.J. Zou, Phys. Rev. D **70**, 094008 (2004).
  - [27] S. Eidelman et al. (Particle Data Group), Phys. Lett. B **592**, 1 (2004).
  - [28] K. Inoue, A. Kakuto, H. Komatsu and S. Takeshita, Prog. Theor. Phys. **68**, 927(1982); *ibid* **71**, 413(1984);
  - [29] M. Kabayashi, T. Maskawa, Prog. Theor. Phys. **49**, 652 (1973).
  - [30] A. Djouadi, J.L. Kneur and G. Moultaka, <http://w3.lpm.univ-montp2.fr/~kneur/Suspect/>, hep-ph/0211331.
  - [31] G. Buchalla, A.J. Buras and M.E. Lautenbacher, Rev. Mod. Phys. **68**, 1125 (1996).
  - [32] C. Bobeth, T. Ewerth, F. Krüger and J. Urban, Phys. Rev. D **66**, 074021 (2002).
  - [33] Gi-Chol Cho, K. Hagiwara, Nucl. Phys. B **574**, 623 (2000).
  - [34] J. Ellis, S. Heinemeyer, K.A Olive, and G. Weiglein, JHEP 0502, 013 (2005); S. Heinemeyer, W.Hollik and G. Weiglein, hep-ph/0412214;
  - [35] For more details of SPA project, see SPA home page: <http://spa.desy.de/spa/>.
  - [36] B.C. Allanach *et al.*, Eur. Phys. J. C **25**, 113 (2002).
  - [37] P. Gambino, U. Haisch and M. Misiak, Phys. Rev. Lett. **94**, 061803 (2005).
  - [38] A. Ali, E. Lunghi, C. Greub, and G. Hiller, Phys. Rev. D **66**, 034002 (2002).
  - [39] H.H. Asatryan, H.M. Asatryan, C. Greub, and M. Walker, Phys. Lett. B **507**, 162 (2001).
  - [40] Belle Collaboration, K. Abe, et al, hep-ex/0508009.
  - [41] H.Y. Cheng and Kwei-Chou Yang, Phys. Lett. B **511**, 40 (2001); Y.D. Yang, R.M. Wang and G.R.Lu, Phys. Rev. D **72**, 015009 (2005).
  - [42] Heavy Flavor Averaging Group, <http://www.slac.stanford.edu/xorg/hfag>.
  - [43] A. Ali, J. Chay, C. Greub and P. Ko, Phys. Lett. B **424**, 161 (1998).
  - [44] A.L. Kagan, Phys. Lett. B **601**, 151 (2004).
  - [45] M. Bauer, B. Stech, and M. Wirbel, Z.Phys. C **34**, 103 (1987);
  - [46] P. Ball and R. Zwicky, Phys. Rev. D **71**, 014029 (2005).